6-2011

Expression Level of Kita, Kitb, Kitla, and Kitlb in Zebrafish Gastrointestional Tract

Jennifer B. Strouse
The College at Brockport

Expression Level of Kita, Kitb, Kitla, and Kitlb in Zebrafish Gastrointestional Tract

By

Jennifer B. Strouse

To

Graduate School in Partial Fulfillment of the Requirement for the Degree of Master of Science in Biological Sciences

The College at Brockport

June 2011

THESIS DEFENSE

APPROVED	NOT APPROVED	MASTER'S DEGREE ADVISORY COMMITTEE	
✓		Major Advisor	Date: 7 June 2011
✓		Committee Member	Date: 6/7/11
✓		Committee Member	Date: 6/7/11

Chairman, Graduate Committee

Chairman, Dept. of Biological Sciences

Abstract

Gastrointestinal (GI) motility is the muscular contractions that move intestinal contents in an anterograde (mouth to anus) direction and is necessary for nutrient absorption and elimination of waste. GI motility is highly coordinated and rhythmic contraction patterns. Interstitial cells of Cajal (ICC), enteric neurons, and smooth muscle cells all regulate GI motility. ICC function as pacemaker cells and determine contraction frequency. ICC growth and development is influenced by Kit, a tyrosine kinase receptor located on the plasma membrane of ICC. TMEM16A is a calcium activated chloride channel which contributes to the slow wave in the GI tract. Constipation, delayed gastric emptying, and bloating have been correlated with deficits of ICC in GI tissues.

A functional Kit receptor and stimulation of Kit with Kit ligand is necessary for ICC growth and development. However, little is known about ICC development in adults or in developing GI tissue. The objective for this project is to determine the relative and temporal expression levels of Kita, Kitb, Kitla, and Kitlb in the zebrafish model system at several developmental time points. Understanding the temporal and relative expression pattern of these genes is the first step towards a more complete understanding of ICC development and turnover.

The zebrafish model system is anatomically similar to the human GI tract and at early time points the zebrafish is transparent. One advantage to this model system is that GI motility may be examined in the intact larvae. RNA was isolated from dissected zebrafish GI tissues and used as template for reverse transcriptase reactions to make cDNA. Relative and temporal expression levels of Kita, Kitb, Kitla, and Kitlb was determined at 5 days post fertilization (dpf), 7dpf, 11dpf, 28dpf, and in adult gut tissues using cDNA as template for real time PCR.

Kita and Kitla were confirmed as a functional receptor/ligand pair which was first identified in melanocyte migration[19]. The relative expression data suggests that Kitb and Kitlb are also a functional receptor/ligand pair. Temporal expression data shows high expression of Kitb early in development (5dpf). Besides the early high expression of Kitb, gene expression for all genes of interest peak at 11dpf.

TMEM16A (also called ANO1) was identified as a more accurate marker for gastrointestinal stromal tumors (GIST) than Kit[24]. RNA isolated from dissected zebrafish GI tract was used to make cDNA which became the template for reverse-transcriptase (RT)-PCR and real-time PCR (q-PCR). Anti-ANO1 antibodies were used to identify TMEM16A in dissetcted, fixed zebrafish GI tract.

RT-PCR showed that TMEM16A, B, and C are expressed in the zebrafish GI tract. Immunohistochemistry identifies a network of cells in the zebrafish GI tract that is similar in morphology and location to ICC stained by Kit antibodies. Relative and temporal expression was determined using samples isolated at 5, 7, 11, 28dpf, and adult time points. Expression of TMEM16B dominates TMEM16A and B at 28dpf and adult time points.

Table of Contents

Appendix

List of Figures

Real-Time PCR

TMEM16A is Expressed on Zebrafish ICC

Kit/Kitl

Acknowledgments

I thank Dr. Rich for his support and guidance with this project and as an advisor, Dr. Sia and Dr. Pelletier for their assistance as committee members, and fellow lab members for help in running experiments and raising/caring for fish, especially Jessica Ouderkirk.

Specific Goals of the Research

The purpose of this study is to measure the relative and temporal expression of genes involved in growth, development, and maintenance of interstitial cells of Cajal (ICC). The genes of interest are Kita, Kitb, Kitla, and Kitlb. This study will contribute to knowledge of ICC and the relationships between the genes in the zebrafish gastrointestinal (GI) tract. Real-time PCR(q-PCR) was used to determine the relative and temporal expression of Kita, Kitb, Kitla, and Kitlb in the zebrafish GI tract at 5 days post fertilization (dpf), 7 dpf, 11 dpf, 28 dpf, and adult time points. Analysis of raw C_q data from real-time PCR resulted in normalized data when compared to reference gene data and relative/temporal expression when compared to calibrator data.

This thesis also contains data pertaining to a novel marker for ICC, TMEM16A, which contributes to the slow wave and thus plays a role in contraction on GI smooth muscle. TMEM16A was positively identified on zebrafish ICC through immunohistochemistry, reverse transcriptase (RT)-PCR, and q-PCR. Orthologs to TMEM16A, TMEM16B and TMEM16C were also identified in the zebrafish through bioinformatics. RT-PCR confirmed the expression of all three genes in the zebrafish GI tract and q-PCR was used to determine relative and temporal expression of these genes.

Introduction

The gastrointestinal (GI) tract includes the mouth, esophagus, stomach, small intestine, large intestine, and the anus. It can be thought of as a tube, approximately 30 feet long in an adult human, which separates the intestinal contents from body fluids. The function of the GI tract is to digest food, absorb nutrients, and eliminate wastes. GI tract anatomy is layered and moving from the body side (serosa) to the inside of the GI tract (lumen) is comprised of layers of smooth muscle cell, connective tissue (mucosa) and an inner epithelial layer. Smooth muscle cells grind and mix ingested food into a slurry (chyme) to facilitate digestion. The chyme is moved forward in an oral-to-anal direction, also called the anterograde direction. This process is highly regulated to achieve a balance between efficient nutrient absorption and elimination of waste. Contraction of smooth muscle along the long digestive tube is therefore highly coordinated and GI motility describes this process. Three cell types contribute to GI motility; smooth muscle cells, enteric neurons, and interstitial cells of Cajal (ICC), and these three cells together are called the intestinal triad. Each cell type is necessary for spontaneous, rhythmic coordinated GI motility patterns to occur. This thesis focuses on genes that influence ICC growth and development.

Disruption of any single component of the intestinal triad will result in a decreased coordination of smooth muscle contractions, and GI dysmotility occurs. There are many forms of dysmotility in humans, ranging from acute diarrhea and constipation, to chronic diseases such as irritable bowel syndrome (IBS) and inflammatory bowel disease (IBD). GI dysmotility can also be a side effect of other diseases such as diabetes. Dysmotility is usually accompanied by a reduction in ICC; Nakahara et. al showed that patients with diabetes mellitus had 40% less kit-positive cells (ICC) compared to non-diabetic patients. Infants with small bowel atresia (closure of the small intestine), were found to have significantly less ICC then infants with no obstruction[40]. Approximately 25% of adults experience GI motility disorder[32]. It is important to understand the regulation of GI motility and to search for novel treatments because the quality of life for GI dysmotility patients can be greatly affected. A societal burden is also created by GI motility disorders because patients report missing work. Understanding the physiological disruption that causes dysmotility may aid the diagnosis and proper treatment GI problems. Determining expression patterns of genes that are required for ICC growth and maintenance will

contribute to the understanding of ICC growth at the molecular level and may contribute to eventual treatment options for GI dysmotility.

ICC Morphology, Anatomy, and Function

ICC are necessary for the spontaneous rhythmic contraction of the GI tract. ICC were first identified by Ramon y Cajal in 1911 when he reported nerve-like cells at the ends of motor neurons in organs innervated by peripheral nerves. ICC are now identified using antibodies to the Kit protein which is expressed on the ICC cell surface but is not expressed in other cells within the GI tract[37]. ICC are large cells which typically have multiple branches extending 200 μm or more, a large cell body, and are more similar in appearance to neurons which also display multiple branch points compared to smooth muscle cells that are typically bipolar. ICC develop from the mesoderm, the same lineage as smooth muscle, and are therefore distinct from neurons[22]. Individual ICC may be observed in the circular muscle layers of the GI tract but the majority of ICC form a network of cells between the circular and longitudinal muscle layers, near a network of neurons in the myenteric plexus region. A second network of ICC form a layer in the deep circular muscle close to the submuscosa. ICC in this layer are primarily bipolar and are less dense compared to the myenteric layer of ICC[20, 37]. ICC morphology and location in the zebrafish is similar to humans, but zebrafish ICC are smaller and therefore more difficult to image[35]. ICC morphology is distinct, and is related to function. Myenteric ICC are stellate, with many branching processes, and form a network that is positioned between the circular and longitudinal muscle layers. The stellate morphology and gap-junction connected network of myenteric ICC are ideal for the distribution of the pacemaker signal to the circular and the longitudinal muscle layers. ICC also form gap junctions with smooth muscle cells, allowing transmission of the pacemaker signal from ICC to smooth muscle. However, ICC-smooth muscle gap junctions are smaller when compared to ICC-ICC gap junctions, enabling the ICC to convey information more quickly to each other, and down the long axis of the gut. Bipolar ICC are located within both muscular layers and functionally integrate and amplify neural input. The networking patterns of ICC (bipolar and stellate) allow the cells to communicate not only down the long axis of the gut but also around the circumference, leading to smooth muscle contraction and the propagation of contraction in the anterograde direction[17].

The resting membrane potential of ICC slowly oscillates and this pattern is called the electrical slow wave[48]. ICC form gap junctions with smooth muscle cells allowing the flow of electrical current between ICC and smooth muscle, and therefore

the slow wave that originates in ICC is transmitted to smooth muscle cells. The resting membrane potential of smooth muscle cells slowly oscillates, following the ICC slow oscillations. Contraction of GI smooth muscle coincides with depolarization of the slow wave, and relaxation coincides with hyperpolarization of the slow wave. Therefore, smooth muscle contraction follows the same pattern as the electrical slow wave that originates in ICC[20, 37].

The Role of the KIT Gene

The KIT gene encodes a receptor tyrosine kinase that regulates cell growth in a variety of cell types, including hematopoietic stem cells that are essential for red blood cell synthesis, melanocytes which are involved in pigmentation, and ICC, which are required for GI motility. The Kit protein is located in the plasma membrane of ICC and is the most commonly used marker for ICC identification[22, 28, 37]. There is an extracellular, trans-membrane, and intracellular domain to the receptor. The ligand for the Kit receptor (kitl) binds to the extracellular component of Kit and, when bound, activates an internal cascade leading to cell differentiation and growth. In the GI tract Kit is expressed on ICC and on mast cells. Mast cells are ≈10 μm in diameter and are round whereas ICC are much larger (≈200 μm long) and have multiple processes. Therefore ICC and mast cells are easily differentiated based on cell morphology[27]. Kit function is required for ICC growth and for maintenance of the ICC phenotype. Knockout of the Kit gene in the mouse model results in a complete absence of ICC. Kit knockout mice also display uncoordinated GI contractions, consistent with a functional requirement for ICC[18]. Reduced ICC density is also associated with GI dysmotility in humans[22, 28, 40]. The receptor tyrosine kinase inhibitor imatinib mesylate (Gleevec®) blocks Kit function, and results in the disappearance of ICC and uncoordinated GI contractions in adult mice[38]. This thesis focuses on the temporal expression pattern of the KIT gene and the KIT ligand gene from early development through adulthood in the zebrafish GI tract.

A novel gene expressed in human and mouse ICC has recently been identified, TMEM16A[9, 12]. TMEM16A codes for a calcium-activated chloride-selective ion channel located in the plasma membrane of ICC[20, 48]. This protein is of interest for two major reasons: TMEM16A is a novel ICC marker unrelated to Kit, and TMEM16A may contribute to generation of the electrical slow wave which enables the ICC to act as a pacemaker for the gut[17, 20, 48]. There are ten TMEM paralogues in mammals designated tmem16A-H, J, and K[20]. Outside of the GI tract Tmem16 is expressed in epithelial tissues and has been shown to contribute to fluid secretion by these cells[47]. Putative genes encoding TMEM16A, TMEM16B, and

TMEM16C homologs have been identified in the zebrafish genome and we have verified expression of these genes in the zebrafish GI tract. We have also shown that antibodies raised against human Tmem16A identify ICC networks in the zebrafish GI tract (unpublished data). The functional importance for TMEM in the zebrafish GI tract, and on zebrafish ICC development, is unknown. This thesis includes data on TMEM expression as an independent marker for ICC because it may contribute to our understanding of ICC development.

The Zebrafish Model

Zebrafish are genetically and anatomically similar to humans and are emerging as a model system for human biology and human disease. Zebrafish embryos are transparent which allows direct visualization of organ development in intact and unperturbed animals. Development is rapid and a functional 2 chambered heart is observed by 2 days post fertilization (dpf) and a spontaneously contracting GI tract is observed by 5 dpf. Larvae remain transparent for 7-10 days and therefore organ function can be directly observed in intact animals that contain functional organ systems. The role of specific genes can be examined using morpholino knockdown technology whereby expression can be reduced or eliminated transiently during early development, lasting up to approximately 7 dpf. This technology is limited, and normal gene expression gradually returns over time. The zebrafish model has also been used to identify novel genes with forward genetic screens where random mutations are generated and the resulting phenotypes are observed. The sparse mutant was identified in this way; the phenotype was a lack of pigment and pigment migration. After characterization of the Sparse phenotype the underlying genetic mutation was discovered to be a kita null mutation. Work from our lab showed that Sparse displays a distended gut and poorly coordinated GI muscular contractions, in addition to the lack of pigment[35]. The mouse model system also shows a distended GI tract and poorly coordinated muscular contractions when Kit function is compromised, as in the W/Wv mouse[25]. Similarity between zebrafish and mouse model systems with respect to Kit function and GI motility is one piece of evidence that the zebrafish as a good research model for human gastrointestinal physiology. From a practical viewpoint the zebrafish is a good research model because early development is rapid, time until adulthood (adults are fertile) is only 3 months, breeding is relatively easy and produces large clutches, housing requires little space when compared to mouse models, and feeding costs are low. The ability to directly observe GI motility in intact larvae with fully-developed GI tracts is an advantage in the zebrafish model system that is not present in the mouse model system.

Zebrafish ICC

GI motility in humans is regulated by 3 cellular components: ICC, enteric neurons, and smooth muscle cells. These three cell types are present in the muscularis externa of the zebrafish GI tract and are arranged in layers, similar to humans[35, 43]. The GI tract is sometimes described as a digestive tube with concentric tissue layers. The zebrafish GI tract is anatomically similar to the human and mouse with an inner mucosa and epithelial layer and an outer muscular layers. Moving outward, the muscular layers are the circular smooth muscle layer and an outer longitudinal layer. The myenteric plexus region separates the muscle layers and contains enteric neurons and ICC which functionally regulate muscular contractions[35, 43]. The zebrafish GI tract does not have a region with an acidic pH, or sphincters separating functional regions, like the human. The zebrafish does have a region with an expanded lumen, the intestinal bulb, which displays mixing movements, and propulsive contractions are initiated distal to this region.

The most important similarity between Zebrafish and human ICC is KIT expression. It is important to know that GI smooth muscle and ICC develop from the same tissue layer, the mesoderm, and are differentiated by Kit expression. The zebrafish expresses two KIT orthologues, Kita and Kitb, and also two KIT ligand orthologues, Kitla and Kitlb. Our lab showed mRNA expression of all four genes in zebrafish GI tissues using gene specific primers and polymerase chain reaction. Protein expression of kita and kitb was confirmed using anti-Kit antibodies on fixed, intact tissues. Two types of zebrafish ICC were observed, stellate and bipolar. ICC with multiple processes were primarily in the myenteric plexus region, and bipolar ICC were in higher density near the submucosal border, similar to the mouse and human[35]. It is well known that KIT function is necessary for ICC development and for maintenance of the ICC phenotype in adult tissues[18, 22, 44]. It is also well known that Kit ligand is necessary for KIT signaling in human GI tissues, and therefore a deficit in Kit ligand will reduce ICC density, and this is accompanied by GI motility dysfunction[6].

The cellular and molecular mechanisms regulating ICC development, growth, and survival are unknown. The purpose of these experiments is to measure the relative expression levels of genes that are likely to influence ICC turnover. It is anticipated that genes with high relative expression levels are functionally important for ICC. The temporal expression pattern was also measured for each gene. It is possible that any single gene may be functionally important for ICC development at a distinct developmental time point. Temporal expression patterns may also contribute

to the understanding of gene interactions during development. More specifically, temporal expression patterns may clarify interactions between kit and kitl orthologues. For example, it is not known if Kita is stimulated by Kitla, Kitlb, or both. Determining expression patterns of genes that are required for ICC growth and maintenance will contribute to the understanding of ICC growth at the molecular level and may contribute to eventual treatment options for GI dysmotility.

The aim of this experiment is two-fold; the first aim is to determine the relative expression of each gene at a given time point. The genes of interest are kita, kitb, kitla, kitlb, and SM-22. The chosen time points are 5dpf, 7dpf, 11dpf, 28dpf, and adult. The second aim is to determine the temporal expression patterns for each individual gene. This data may identify if the expression of the receptors can be correlated to the ligand expression in anyway. Using real-time reverse transcriptase polymerase chain reaction (q-RT-PCR) we have identified the expression levels of the kit receptor, ligand, and smooth muscle genes normalized to reference genes; beta-actin, EF1alpha, and Rpl13alpha, and relative to either adult samples (relative expression) or SM-22 (temporal expression). The q-RT-PCR assay offers sensitive quantification of expression which is needed because the amount of RNA in our samples is small. Fluorescence is measurements after each cycle of PCR. The fluorescence is generated by the binding of SYBR Green to double-stranded (ds) DNA, therefore amplicon production increases the fluorescence. The measurements are taken in "real-time" after each cycle and the point at which the signal is higher than the background signal is the data generated for the user called the quantification cycle (C_q value). At the C_q value the PCR reaction is in the exponential phase, if the reaction is working perfectly, this stage will create a doubling of amplicons in each cycle. In conventional PCR the data is gathered in the plateau phase of the reaction where the efficiency of the reaction is decreased due to limited reactants. An additional benefit of q-RT-PCR, compared to conventional PCR is that it allows analysis of data without gel electrophoresis. The efficiency of the reaction is determined by a standard curve. Knowing the efficiency of the reaction and the C_q allows for q-RT-PCR to be quantitative. There is an inherent relationship between the starting copy number and the C_q value. When starting copy number is low, it takes many cycles of doubling for the reaction to reach the threshold and this cause the C_q to be a higher value. Conversely, when the starting copy number is high it takes fewer cycles of doubling to reach threshold and the C_q is low. This allows for determination of starting copy number or relative expression. These experiments use relative expression and require reference genes to normalize the data to. The selection of the reference genes themselves and the number to use for normalization is important and varies depending on the nature of the experiment. The reference genes should have

consistent C_q values between experimental variables. A more thorough discussion of q-RT-PCR follows; however, it is introduced here because the technique allows the sensitivity needed to address the aims of this thesis.

The following contains the complete explanation of theory and methods utilized to complete this thesis. The aim was to determine the relative and temporal expression of genes which influence ICC development and maintenance, in hopes of broadening the scientific communities understanding of this subject.

Experimental Procedures

A brief description for techniques used in this thesis is provided. Detailed protocols are provided in the Appendix.

Aquaculture

Wild-type zebrafish (ZFIN ID ZS6919) obtained from the Zebrafish International Resource Center (ZIRC) and maintained according to standard guidelines in accordance with IACUC guidelines. Fish were maintained at 28°C in system water comprised of reverse osmosis water supplemented with 240mg/L Instant Ocean salts and 75 mg/L $NaHCO_3$. System water was replenished continuously at a rate that was sufficient to replace 20% each day, pH was maintained at ≈7.2±0.2, and conductivity was maintained at ≈1000 ±15 ppm. Adult zebrafish were fed 3 times daily, alternating dry feed (Scientific Hatchery Diet, Aquaneering, San Diego, CA) with live brine shrimp. Dehydrated decapsulated artemia cysts were purchased and cultured daily (Seahorse Source, Fort Pierce, FL). Zebrafish were maintained on a 14-hr/10-hr light/dark cycle. Crosses were performed in the morning and embryos were maintained in embryo medium described in The Zebrafish Book, and incubated at 28°C[31, 46]. Larvae were fed hatchfry encapsulation, grade 0, beginning at 5 days past fertilization (dpf), and live brine shrimp after 11dpf.

RNA isolation

Total RNA was prepared from intact zebrafish larvae and from freshly dissected GI tissues of wild-type zebrafish at 5 days post fertilization (dpf), 7dpf, 11dpf, 28dpf, and adult (4-10 months), using the RNeasy Plus Mini Kit (Qiagen, Chatsworth, CA). Dissected tissues were placed into *RNlater* and RNA isolation was performed within 7 days. First strand synthesis was performed using random hexamer primers and the Verso cDNA Kit (Thermo Scientific, Surrey, UK).

Quality Control

RNA quality influences q-PCR and therefore RNA quality must be determined for each RNA isolation performed. A 5µl aliquot was removed from each total RNA isolation sample and both the aliquot and the 5µl aliquot were stored at -80°C. RNA aliquots were tested for quality using an Agilent Bioanalyzer at the Functional Genomics Center, University of Rochester, Rochester, NY. These results are provided in Appendix 4.

Reverse Transcriptase Polymerase Chain Reaction

Several q-PCR primers were designed for each gene of interest using Primer3 software (http://frodo.wi.mit.edu/primer3/). Product size was constrained between 100 and 200 base pairs. Primers were ordered from IDT (San Diego, California). Each primer pair was tested in reverse transcriptase PCR experiments to verify amplication of a product of the expected size. These experiments were performed using using BioMix Red (Bioline, Laboratory product Sales, Rochester, NY) with 1ul of wild-type, adult zebrafish cDNA as template, 1 μl of a forward and reverse mixture of PCR primers (20 μM each), and run for 35 cycles. Amplification products were resolved on a 2% agarose gel. PCR products were sequenced to verify specificity (Roswell Park, Buffalo, NY).

Real Time quantitative Polymerase Chain Reaction

After primers showed successful amplification of a product with an expected size, optimization for q-PCR experiments was performed. Each primer pair was run on a temperature gradient to determine optimal annealing temperature. Specificity of product was checked by including a melt-curve in the PCR protocol. Optimal temperature for each primer set was determined. A single optimal annealing temperature suitable for all genes was determined and one primer pair was selected for each gene. When examining multiple genes it is essential that primers have highly similar efficiencies. A standard curve for each primer set was created to determine efficiency. Serial dilution of a gene-specific cDNA template was performed and a standard curve was created, from which PCR efficiency is calculated. All primer sets used had efficiencies of 80-120%. A melt curve was part of the PCR protocol for standard curves also to insure the specificity of the reaction.

The relative expression level for each gene was determined in each sample. Samples were comprised of total RNA isolated from GI tissues dissected from at 5, 7, 11, 28 dpf, and adult zebrafish. The temporal expression of each gene was determined as well as the relative expression level between genes at individual time points. The selection of reference genes is extremely important for q-PCR experiments. Ideal reference genes for this experiment would be insensitive to development. Reference genes that are development-insensitive are unknown for the zebrafish model system[41]. Therefore a panel of reference genes was utilized and included β-actin, RPL13α, and EF1α. A MyiQ cycler (BioRand, Hercules, CA) and iQ SYBR Green Mastermix (BioRad, Hercules, CA) were used with a 40 two-step PCR cycle. A melt curve and one serial dilution/standard curve was included in every plate to assay specificity and to verify that the machine and the mastermix was performing as expected. The serial

dilution curve is also necessary as an interplate calibrator, a requirement when comparing q-PCR results from separate experiments.

Data Analysis

q-PCR experiments yield a C_q value for every reaction. Normalized expression levels are calculated by comparing the C_q value for the gene of interest to a reference gene. An ideal reference gene will not change expression under the experimental conditions. For this thesis the experimental condition is the developmental time point. Because an ideal reference gene was unavailable we used a calculated reference gene C_q based on the average C_q for three distinct reference genes; β-actin, RPL13α, and EF1α. The normalized expression level was determined by first calculating a delta C_q value for every gene.

$$\text{Delta } C_q = C_q \text{ (gene)} - \text{Average } C_q\text{(reference)}.$$

Delta C_q is used to calculate normalized expression (NE).

$$NE = 2^{\text{Delta Cq}}$$

Relative expression levels for a gene are calculated using NE for a gene and a calibrator sample. Calibrator samples are the control sample that is used for comparison. Relative expression for multiple genes at single time points used SM-22 expression as the calibrator. SM-22 is expressed by gastrointestinal smooth muscle and was selected as a calibrator so that gene expression can be compared. Temporal expression of each gene used adult gene expression as the calibrator.

Relative expression = NE (experimental sample) / NE (calibrator sample).

Real-Time PCR

Real-time PCR (q-PCR) was first introduced in 1993[15] and has rapidly become a standard technique used to quantify mRNA expression levels. The technology is enabled by the availability of q-PCR machines that are thermal cyclers combined with imaging technology that captures a fluorescent signal in each reaction tube for every cycle. Although q-PCR is faster compared to conventional PCR because end point analysis is not necessary (i.e. agarose gels are not necessary), the primary advantage is that q-PCR is that it is quantitative.

Conventional PCR amplifies a specific nucleotide sequence from a template. The goal for this thesis is to measure gene expression and therefore messenger RNA (mRNA) is the template. Specificity is the hallmark of PCR and is the result of oligonucleotide primers annealing to specific and unique template sequences. After the primers anneal to the template, an enzyme (taq polymerase) creates a copy of the template that lies in between the primers during the PCR cycle. Therefore the copy, or product, of each PCR cycle is a specific length. It is important to know that during each PCR cycle every template is copied, and therefore the total amount of PCR product doubles with each cycle. This doubling represents exponential growth of PCR product. The combination of specificity and amplification result in the power of PCR.

Real-time PCR is also called quantitative PCR. Specificity and amplification in q-PCR are identical to conventional PCR. The quantification step in q-PCR occurs in each cycle and is measured using fluorescence. Fluorescence signal increases as the number of amplicons increase. In our experiments SYBR green dye is used. Free SYBR green molecules have minimal fluorescence, and when bound to double-stranded DNA fluorescence increases 1,000-fold[5]. Therefore, fluorescence signal is proportional to the amount of double stranded (ds) DNA. With every PCR cycle the fluorescent signal will increase, as long as amplicon numbers increase. Because SYBR green intercalates non-discriminately, amplicon lengths must be standardized for different q-PCR reactions, and multiplexing (amplification of multiple sequences using several primers sets) is not possible. The starting copy number or the relative expression level of a gene can be determined using q-PCR. The copy number is the number of template pieces, or mRNA molecules that result from gene expression. From a technical viewpoint, in our lab q-PCR is performed on complementary DNA (cDNA), which is produced from total RNA using reverse transcriptase, not the RNA

itself. Total RNA is isolated from tissue samples. Therefore, the SYBR green fluorescent signal measured in each q-PCR cycle results from amplification of a specific template that is selectively identified by oligonucleotide primers. The amplitude of the SYBR green signal grows exponentially because doubling of PCR product occurs at every cycle[5]. This also allows back-calculation of the starting amount of template to determine the starting copy number. Alternatively, two separate PCR reactions may be compared allowing calculation of relative expression level between two genes. Experiments using q-PCR show the presence of gene transcription and quantifies that expression.

Pitfalls

Real-time PCR is a powerful technique because it utilizes polymerase chain reaction, a well established technique with extremely high sensitivity, and fluorescence chemistry, which also has high sensitivity. q-PCR allows quantification of PCR product which can be related to the amount of starting template. However, there are many potential pitfalls to q-PCR at almost every step in the protocol and care must be taken to minimize and avoid them. The single most important pitfall, for SYBR green technology, is that the fluorescent signal is related to the total amount of dsDNA, regardless of the sequence of that DNA. This means that contamination from genomic DNA, contaminating DNA from a previous experiment, and nonspecific priming or primer annealing to an unintended sequence will yield fluorescent signal that is undistinguishable from intended sequence amplification. Small contamination of starting template from genomic DNA or more commonly, from amplicon contamination from a previous experiment, can be amplified and may dominate the fluorescent signal. Amplicon contamination refers to PCR product from a separate experiment mixing with starting template. Selecting an appropriate reference gene is a significant challenge[41, 42]. Reference gene expression should remain constant with treatment for studies reporting relative expression levels like ours. The ideal reference gene for developmental studies has yet to be found. One approach to solve this problem is to use a combination of reference genes. For these studies 7 reference genes were examined and 3 were chosen because of consistent expression through the chosen developmental time-points used in these experiments (Figure 1) The chosen reference genes were also validated for developmental time course studies[41].

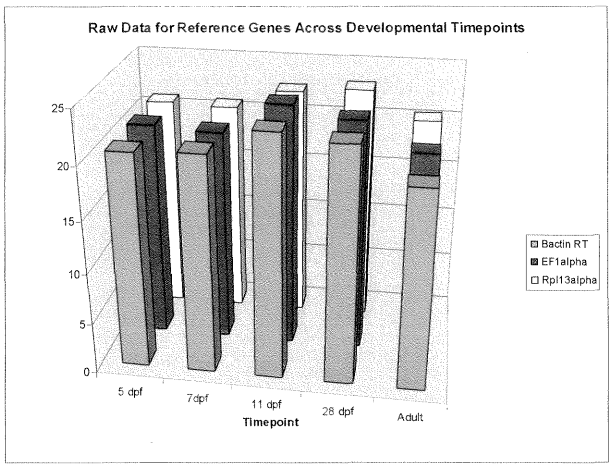

Figure 1 shows the raw C_q values for the three chosen reference genes used to normalize the data in these experiments. The genes used are Beta-actin, elongation factor, and ribosomal protein which were validated in the literature for developmental time course experiments. All three genes show consistent expression when compared to each other and across developmental time-points (C_q within five cycles).

RNA Quality

RNA quality is the first pitfall in every q-RT-PCR reaction and can affect the reliability of the results. The transcriptome, all of the different expressed mRNA, reflects the pattern of gene transcription and is easily degraded when compared to the genome. Therefore it is critically important to measure the quality of isolated RNA to get consistent and reliable results. RNA must be of good quality from isolation to reverse-transcription (RT). The best way to determine quality of RNA is inspection of 28S and 18S ribosomal RNA bands using gel electrophoresis or more automated methods such as Agilent's RNA LabChip and 2100 Bioanalyzer. The 2100 Bioanalyzer is useful when routinely analyzing large numbers of RNA samples because it assigns an RNA Integrety Number (RIN) to each sample, ranging from 0 – 10 with 10 being an undegraded sample and zero being a very degraded sample. The 2100 Bioanalyzer system also generates an artificial gel to show the 28s and 18s peaks/intensity as a band (Data shown in appendix). Quality RNA shows strong 28s and 18s ribosomal RNA bands reflecting minimal degradation[7, 8]. Another important aspect of RNA which will be used for q-PCR is that it be DNA free which is even more important if the amplified gene is free of introns. If DNA contamination is present it will show on the gel as multiple bands or a smear above the 28s band. Whenever possible, primers for our studies span intron-exon boundaries minimizing effect of DNA contamination. DNA contamination in this case is indistinguishable from RNA and will skew the quantification. RNA isolation should not purify inhibitors of the RT step along with the RNA. Inhibitors of the RT step include heme and calcium, and therefore care should be taken to remove these contaminators. RNA should be free of nucleases because nucleases degrade the sample while in storage. A sample with significant RNA degradation will show multiple or blurred bands at the 28s and 18s markers as well as multiple bands/smears that are small in size (seen at

the bottom of the gel). Finally, the storage and treatment of RNA samples also affects the quality. Degradation is minimized when samples are stored at -80°C in small aliquots and the number of freeze/thaw cycles the sample is exposed to is minimized.

Specific Vs. Non-specific Chemistries

SYBR green q-PCR is a non-specific chemistry because it reports double stranded DNA amount, regardless of the sequence. Specific chemistries, like a Taqman probe, requires design of a third primer set which anneals between forward and reverse primers on the template. The third template contains a fluorescent molecule and a quencher. The quencher prohibits fluorescence when primers are intact. As Taq polymerase reads the template the third primer is degraded, both the fluorescent molecule and quencher molecule is released from the primer, resulting in a fluorescence increase. The use of the third primer makes the design of this experiment specific because the primer with fluorescent probe will only anneal on the sequence being amplified and thus fluorescence will occur only when the sequence of interest is amplified. This technique allows multiplexing, or many simultaneous experiments run in a single well, because each probe can contain a different fluorescent molecule[8]. SYBR Green is a fluorescent molecule that is activated when it intercalates with double stranded DNA[5]. The more double stranded DNA present in a sample the more molecules of SYBR Green that will intercalate with DNA, generating more fluorescence. SYBR Green intercalates with any double stranded DNA and if DNA contamination or non-specific priming occurs the results will be unreliable. One safeguard against contamination is the melt curve. Melt curves show the temperature at which double stranded DNA denatures, or melts, and the melting temperature is length dependent and partially sequence-dependent. Melt curves for each PCR reaction indicate the presence of one or several amplicons.

Linearity

Real-time PCR assumes doubling of PCR product for every cycle, according to the equation

$$\text{Copy number} = \text{Copy number}_{start} * 2^n$$

Where n is the number of PCR cycles. When n = 0 the copy number is the amount of starting template and as n increases the copy number doubles with each cycle. Doubling of PCR product doesn't always occur because PCR amplification is not always 100% efficient. Therefore PCR efficiency must be measured for every primer pair using a standard curve. A standard curve is generated using a serial

dilution of template for every primer pair and the resulting efficiency, typically between 90 and 110%, is used when analyzing data[5]. Plotting fluorescence intensity versus cycle number results in a sigmoid curve, where exponential increases in fluorescence are observed in the mid range of the curve. During early PCR cycles the florescent signal is below detection, and therefore the slope of the curve is small and the fluorescence represents background. An inflection point is obvious when the slope increases, and at this point exponential growth of fluorescence begins. This point is the quantification cycle. The quantification cycle is typically the earliest PCR cycle when fluorescence is clearly above background levels[5, 8]. After many PCR cycles efficiency drops dramatically because Taq efficiency declines and/or substrate concentrations become limiting. At high cycle numbers fluorescence intensity does not increase, the slope of the curve is small, and this indicates that PCR amplification is no longer exponential (Figure 2).

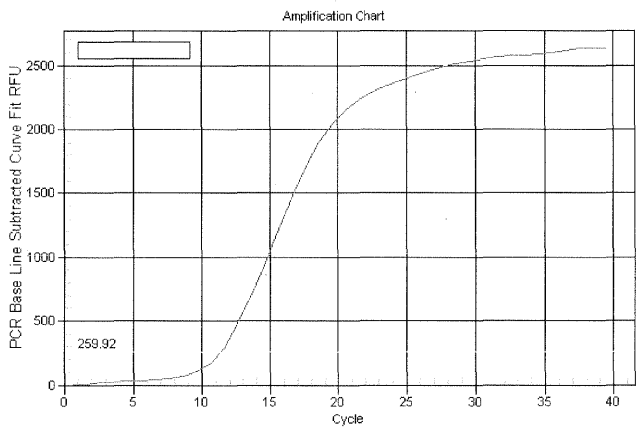

Figure 2 shows a typical amplification curve in a q-PCR reaction. The red line shows an increase in fluorescence which is slow at first then more dramatic after crossing the quantification cycle (yellow line). The assay design of q-PCR allows for a direct correlation between increased fluorescence and increased amplicon. The amount of amplicon produced each cycle levels out in the later cycles due to enzyme inefficiency and lack of reagents. This is seen in the plateau at the end of the reaction.

Data Analysis

Real-time PCR results in a fluorescent intensity value for every well in the PCR plate. There are 96 wells per plate. Fluorescent intensity is expected to reflect copy number of the gene of interest in each well, but many other factors can influence fluorescent intensity. Simple issues like pipetting error are possible. The solution is practice, performing every reaction in triplicate, and dedicating a set of recently-calibrated pipettes for q-PCR experiments. Performing experiments in triplicate gives more confidence in results because outliers can be identified, and discarded. PCR efficiency in every experiment can be influenced by a particular batch of SYBR green

or Taq polymerase, making comparison between experimental plates difficult. The solution is to run a standard curve using a selected primer pair for the experiment on every plate so that efficiency can be calculated and compared[5]. Similarly, fluorescent intensity for excitation and the fluorescent detection efficiency may change between experiments. The solution is to use a standard curve on every plate and compare this standard curve to the original standard curve ran for the gene on the plate. This compression shows if the reaction is working at a similar efficiency as prior experiments. If efficiency is outside of normal ranges then the thermal cycler should be calibrated. If the problem persists then new batches of reagents should be used. Real-time data will also be influenced by differences between biological samples. Differences in RNA isolation quality between samples can yield vastly different results in q-PCR reactions because the samples will have varying amounts of starting copy number. RNA isolation from tissues of varying size will also have differences in starting copy number, and thus, in q-PCR results. In both cases gene expression would appear to be higher in one sample though it is not correlated to the transcriptome profile. Therefore reference genes are used to normalize every sample. Reference gene expression would mimic the expression levels in both the poor isolation and larger amount of tissue examples. When data is normalized to the reference gene the potential for error is minimized and the potential to identify physiologically significant gene expression patterns is maximized.

Consistency of reagents

Real-time PCR quantification relies heavily on consistent reaction efficiency as described above. The efficiency of a reaction is determined primarily by the enzyme's ability to catalyze the reaction and secondly by the availability of substrates and absence of inhibitors. The more consistent the reaction mix is, including each individual reagent, the more consistent the efficiency will be between reactions. If efficiency is consistent than data analysis is more accurate.

Analytical methods

Real-time PCR experiments report absolute expression or relative expression for a specific gene. The decision to calculate absolute or relative expression is made before the experiment is performed. Absolute expression analysis requires construction of a standard curve using serial dilutions of the gene of interest. C_q is compared to a standard curve, and the starting copy number is calculated. It is appropriate to use absolute quantification when the sample of interest doesn't rely on any other sample. The BIORAD applications guide gives this example: An example of when to use absolute quantification would be if a doctor was interested in the

number of virus particles per ml of blood in a patient. The patients sample is compared to a standard curve of known amounts of virus particles. Note that the patient's results don't rely on any other sample to draw a conclusion.

Relative expression analysis typically compares two samples. Expression of the gene of interest in the experimental sample is reported relative the expression of the same gene in a control sample. Gene expression in each sample must be normalized before relative expression between samples is calculated. The BIORAD application guide gives this example: relative quantification would be used if a researcher is interested in whether a receptor expression changes between cancerous and non-cancerous cells. The cancer cell receptor expression levels have to be compared to the normal cell receptor expression levels in order to conclude anything about the receptor expression.

Absolute and relative quantification both require a normalizing agent which ensures that the data is biologically meaningful. Normalizing agents are used in absolute quantification to standardize the target quantity to the unit amount of sample. In the viral particles example the normalizing agent is ml of blood. Other normalizing agents commonly used for absolute quantification are number of cells and μg of nucleic acid used. For relative quantification reference genes are used as normalizing agents. A good reference gene will not change expression with treatment and allows the researcher to account for differences in sample sizes by normalizing C_q data for the samples to C_q data for the reference genes[41].

Standardization of protocols (MIQE)

One of the major difficulties with q-PCR is confidence in data reported because until recently there was no standard for experiments or publications. In 2009, The MIQE (pronounced *mykee*) Guidelines were proposed[7]. This document suggested standards for nomenclature, including the abbreviation q-PCR as opposed to RT-PCR for "real-time" which is easily confused with reverse-transcriptase PCR. Terms commonly involved in q-PCR experiments and publications are defined so that these terms are used correctly and consistently. The bulk of the MIQE document concentrates on the items essential to report in publication and suggests how these items might be done; one example is sample extraction, storage and quality. This disclosure allows for reproducibility of experiments and data analysis evaluations, so that methods can be scrutinized for appropriateness and accuracy. Following the MIQE guidelines helps to strengthen the power of q-PCR by making the data and publications more reliable, and helps researchers avoid many common pitfalls

associated with q-PCR. This thesis conforms to the MIQE guidelines given in Table 1 of the MIQE publication[7].

Confidence in Results

Potential pitfalls are considered before running an experiment so that reliable data result. After an experiment is complete it is also important to re-consider potential pitfalls, and how each pitfall could influence experimental results. Only after this analysis can results be interpreted and conclusions developed with reasonable confidence. RNA isolation is the first step in a gene expression study, and RNA quality is critically important. RNA quality was examined in these experiments using Agilent Bioanalyzer. RNA samples with a strong 28s and 18s ribosomal subunit band were used for the q-PCR experiments. DNA contamination was also considered, although small amounts should not affect results because the primer design spans intron-exon boundaries. The amount of RNA used when preparing cDNA should be standardized so that quantified expression levels result from identical amounts of original template. We used 20 ng of isolated total RNA per 20 µl cDNA synthesis reaction for these experiments. Selection of appropriate reference genes is necessary when calculating relative expression values. A literature review is helpful when selecting reference genes, but it is not always possible to find appropriate reference genes for all circumstances and all species. We used a panel of reference genes, some of which were validated for zebrafish time course studies[41]. An additional reference gene, SM22, was selected to attempt to correct for potential changes in gene expression resulting from changes in the mass of the muscularis externa where our genes of interest are expressed. We reasoned that SM22 would help to distinguish changes in gene expression resulting from growth of the outer muscular layers of the GI tract from gene expression due to molecular interactions between Kit and Kit ligand. Experiments are always performed with triplicate samples on each plate to avoid simple pipetteing errors. Scanning the experimental results for obvious outliers in the triplicate samples identifies this error type. Variation in gene expression between individuals is expected. Isolation of RNA from pooled dissected tissues, ≈15 larvae GI tracts, was performed for each time point because individual GI tracts did not yield sufficient RNA for reliable cDNA synthesis. This approach had the additional benefit of eliminating individual differences in gene expression but not interfering with temporal expression patterns. Two approaches were used to avoid plate to plate differences in enzyme efficiency and hardware variations, in particular variation in fluorescence excitation, emission and collection. An entire experiment was run on each plate, examining expression of one single gene at many time points, as well as all reference genes. In addition, a

complete standard curve was run on each plate so that experimental results from several plates can be compared if needed in future experiments.

In summary, q-PCR requires careful planning and analysis because the technique is so sensitive. Validation is necessary at each segment; RNA isolation, primer design, q-PCR execution, and data analysis. A retrospective review of each step at the end is always necessary for full confidence in the data.

The following section describes experiments related to this theses main objective. The body of work was written by Dr. Adam Rich, Department of Biology, College at Brockport. This research was the basis for an Honors thesis written by Jessica Ouderkirk, BS Biology 2010, College at Brockport. The gene comparisons were done by Adam Rich. The immunohistochemistry experiments were done by Adam Rich, Jessica Ouderkirk, and Jennifer Strouse. The image presented in Figure 6 was taken by Adam Rich. The PCR experiments (both conventional and real-time) were run by Jennifer Strouse and Figures 2, 3, 4, and 5 were created by her. Table 2 was also compiled by Jennifer Strouse.

TMEM16A is expressed on zebrafish ICC

Adam Rich, Jessica Ouderkirk, Jennifer Strouse, Simon Gibbons, and Gianrico Farrugia

Introduction

TMEM16A expression is up-regulated in gastrointestinal stromal tumors (GIST), recent work has shown that TMEM16A is a selective marker for interstitial cells of Cajal (ICC) and that TMEM16A plays a role in the electrical slow wave that underlies the spontaneous rhythmic contractions that give rise to gastrointestinal motility[12, 17, 20]. To better understand the physiological role of TMEM16A it is interesting to begin with a summary of the discovery of TMEM16A expression in the GI tract. Several types of tumors occur in the wall of the digestive tract, collectively termed soft tissue tumors, and include GIST, desmoid fibromatosis, Schwannoma, and Leiomyosarcoma (LMS). GIST and LMS are found in the muscular wall of the GI tract and are therefore similar in appearance. LMS originates from smooth muscle hyperplasia and GIST originates from ICC hyperplasia[21]. GIST and LMS are usually identified during endoscopic or radiologic exams and the tumor protrudes, or bulges, towards the intestinal lumen. It is not surprising, given that the tumors originate in different cell types, that treatment for the tumors differs. Diagnosis is critically important for patient survival. Most GIST result from activating mutations in the receptor tyrosine kinase Kit, resulting in Kit over expression, and leading to ICC hyperplasia and tumorigenesis. A definitive GIST diagnosis relies on Kit immunohistochmistry but a small fraction of tumors are missed because some GIST do not over express Kit protein. The inability to diagnosis some GIST motivated the search for a novel marker that positively identifies all GIST[45]. TMEM16A, named DOG1 by West et al, because it was discovered on a collection of tumors termed GIST1, was found to be strongly expressed and universally on GIST. These scientists showed that TMEM16A expression is similar to Kit expression on GIST, but that

TMEM16A was also expressed on Kit-negative GIST. Therefore TMEM16A was identified as a specific, selective, and universal marker for GIST tumors.

Several groups have subsequently verified that TMEM16A, also called anoctamin 1 and DOG1, is expressed on ICC and is a specific and selective marker for GIST[10, 24, 45]. Early work using cell sorting techniques on mouse tissues showed that TMEM16A was expressed 20-fold more abundantly in ICC isolated from the deep muscular plexus 11-fold more abundantly in ICC isolated from the myenteric plexus when compared to the surrounding tissues[9]. The TMEM family contains 10 members that show tissue-specific expression patterns and function as calcium-activated chloride-selective ion channels[13, 17]. Ion channels are necessary for a wide variety of physiologic functions, and TMEM16 calcium-activated chloride channels are functionally important in ICC, photoreceptors, and olfactory neuronal signaling[17]. Diabetic patients with delayed gastric emptying, express different alternative splice variants for TMEM16A when compared to normal controls[26]. The alternatively spliced TMEM16A was also shown to produce less ionic current with slower kinetics[26]. These results show that TMEM16A if functional important in GI motility, and that calcium activated chloride channels influence GI motility. Results from the mouse model system contribute to our understanding of the functional role for TMEM16A in GI motility. TMEM16A knockout mouse display weak and irregular contractions in stomach smooth muscle and the spontaneous, rhythmic oscillations in the membrane potential normally observed in small intestinal smooth muscle are absent in knockout mice[17, 20]. Taken together these data strongly support the presence and functional requirement of a specific TMEM gene, TMEM16A, in gastrointestinal ICC.

Kit-like immunoreactivity has been the most reliable and most commonly used marker for ICC in humans and in all model systems. The Kit protein is a receptor tyrosine kinase that regulates ICC cell development, and is necessary to maintain the ICC phenotype in GI tissues. Kit-like immunoreactivity has also been used to identify zebrafish ICC[36]. The zebrafish model differs from mouse and human in that development of the GI tract can be visualized directly in the intact organism. The GI tract is continuous and spontaneous contractions begin near 4 dpf, and the GI tract appears to be fully functional for nutrient absorption by 7 dpf[43]. Regulation of GI motility by enteric neurons and ICC is intact at 7 dpf when spontaneous contractions appear more regularly and are better organized (A. Rich, personal communication). The GI tract continues to develop functionality after 7 dpf and motility patterns are become increasingly coordinated until 11 or 14 dpf[14] (Adam Rich, personal communication). ICC cannot be directly visualized because there is

one element of a cellular network located within the muscular wall of the GI tract. ICC can be indentified at 7 dpf using anti-Kit antibodies, and both Kita and Kitb mRNA are present earlier, at 5 dpf[35]. A panel of antibodies was tested against zebrafish ICC and one antibody was selective and specific for a network of cells located in the region where ICC are expected to be found, between the circular and longitudinal muscle layers. The cellular morphology of zebrafish Kit-positive cells was also similar to mouse and human ICC. However, the antibody used in those experiments was raised in the rabbit against a human Kit antigen. Therefore, it is possible that the anti-Kit antibody identified a different epitope in the zebrafish. A second, independent ICC marker will verify the presence of zebrafish ICC.

The objective of this work is to determine the expression of zebrafish TMEM16 orthologs and related proteins in zebrafish GI tissues. Potential TMEM orthologs were identified from the National Center for Biotechnology Information (NCBI) CBI and Ensembl databases. A panel of anti-TMEM16A antibodies was tested, using fixation conditions that were identical to those used on mouse and human tissues.

Results

Name	Length	Name	Length	Score
Ano1 human	986	Ano1 Danio	925	63
Ano2 human	1000	Ano2 Danio	452	53
Ano3 Human	983	Ano3 Danio	988	68

Table 1. Clustal W sequence comparisons for 3 zebrafish orthologs.

TMEM16A is specifically expressed in human and murine ICC, and expression is up-regulated on GIST[12, 45]. TMEM16A expression has been shown in epithelial and mesenchymal tissues from the stomach and small intestine of the mouse[13]. TMEM16A is expressed 20-fold more in isolated ICC when compared to smooth muscle cells from the mouse[9]. Therefore we first searched for zebrafish orthologs to TMEM16A and identified zebrafish anoctamin 1 (LOC 407698). The zebrafish orthologue is predicted to code for a 925 amino acid protein, compared to 986 amino acids for human. Comparing the predicted zebrafish protein sequence with human anoctamin 1 protein sequence resulted in a 63% similarity score as seen in Figure 1. Two additional zebrafish anoctamin orthologs that are phylogenetically nearby Anoctamin 1 were identified from the NCBI database, Anoctamin 2 (one branch) and Anoctamin 3 (two branches)[13]. Similarity data are summarized in Table 1.

The possibility that each anoctamin ortholog is expressed in the zebrafish GI tract was examined using reverse transcriptase PCR. Primers were designed to

Name	Sequence (5'-3')	Accession	Tm (°C)	Size (bp)	Date synthesis
TMEM16a3F	AAC GCA AGA TTG ACC CAA AG	NM_001161590 XM_001923853	53.7	504	5-Jan-10
TMEM16a3R	TGC ACG TGT CCA CTT GGT AT		56.7		
TMEM16c3F	CGT CAA TCT CAA CAG CTC CA	XM_001922341	54.9	546	5-Jan-10
TMEM16c3R	ACA GCC ACA ACT CCA ATT CC		55.6		
TMEM16b2F	TCAGGTGGCCAATAACATGA	NM_001110392 XM_689644	54.0	572	24-May-10
TMEM16b2R	AGTGGGTGAGGAACTTGGTG		57.1		

Table 2 shows the primer sequences used in reverse transcriptase PCR for the zebrafish TMEM16 orthologs. Primer name, sequence, accession number, expected melting temperature, expected product size in base pairs, and synthesis date is also shown.

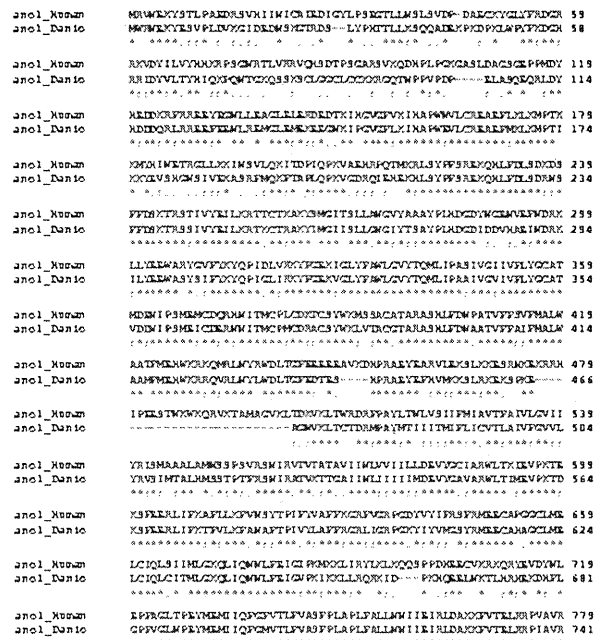

Figure 1. Amino Acid Sequence alignment of human, mouse, and zebrafish anoctamin proteins. ClustalW alignment of zebrafish and human anoctamin proteins. Dashes represent gaps, asterisks indicate identical amino acid residues, and colons designate conservative substitutions. Zebrafish anoctamin 1 showed an alignment score of 63 with human anoctamin 1.

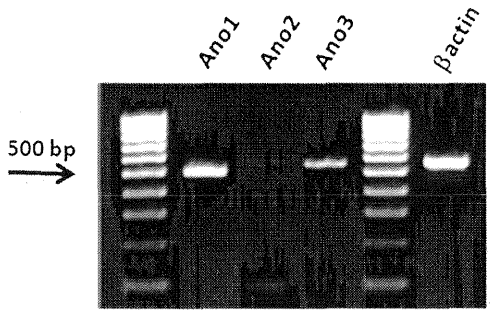

Figure 2. Reverse transcriptase PCR amplifies the zebrafish *anoctamin* 1, 2, and 3 gene products from isolated adult GI tract. Amplicons are shown for primers sets designed for each gene, and for the positive control β-actin. Products of the expected size for each primer set were observed.

amplify specific sequences from each gene. cDNA template was prepared from total RNA isolated from dissected adult zebrafish GI tissues. The results are shown in Figure 2. Primer sequences and expected amplicon size are given in Table 2. Each primer

successfully amplified sequence of the expected size, indicating that all 3 genes are expressed in the zebrafish GI tract. A positive control, beta actin, showed that cDNA template was intact.

Expression of anoctamin 1, 2, and 3 was previously shown in mesenchymal and epithelial tissues from the small intestine in the developing mouse[13]. We used qPCR to examine relative expression levels of the three TMEM16 orthologs in zebrafish adult GI tissue (Figure 3). Surprisingly, these data show that anoctamin 2 expression was 8 fold higher compared to Anoctamin 1. These data suggest that anoctamin 2 is expressed by many more cells when compared to anoctamin 1 and 3, and may indicate epithelial expression. Alternatively, anoctamin 2 may be differentially expressed at higher levels when compared to anoctamin 1 and 3.

We next examined the relative expression level at several developmental time points using q-PCR. Expression of TMEM16A at each time point was used as the calibrator gene. Therefore, TMEM16 B and C are compared to TMEM16A. At 5 dpf expression of TMEM16B and C was 0.85 and 0.80 fold of TMEM16A. At 7 dpf the difference increase modestly so that TMEM16B and C expression are 0.24 and 0.45 fold of TMEM16A. TMEM16B expression increases at 7 dpf and exceeds TMEM16A expression by 1.27 fold. AT 28 dpf TMEM16B expression increases sharply, 8.1 fold increased compared to TMEM16A. This is similar to the increased expression observed in adult GI tissue. A separate experiment was performed to examine the temporal expression pattern for each gene. Expression of each gene was compared to expression level at 28dpf. TMEM16A expression levels rise after 5 dpf rapidly, peaking at 7dpf. Expression of TMEM16B and C rise more slowly and peak at 28 dpf. The functional significance of each gene is unknown at this time.

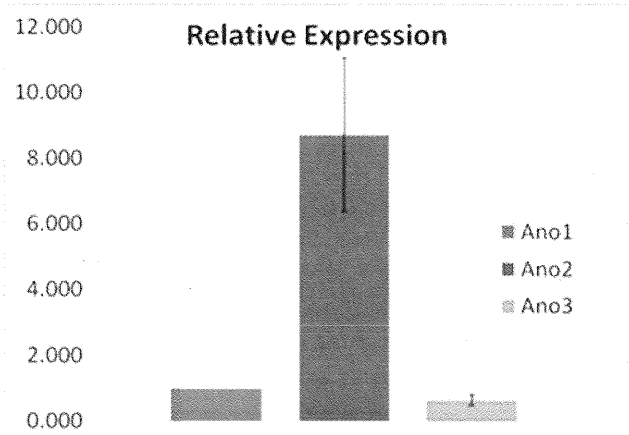

Figure 3. Relative expression level of zebrafish anoctamin 1, 2, and 3 in adult GI tissues. Ano2 was expressed 8.7±2.3 fold more, and Ano3 0.63±0.17 fold less when compared to Ano1 (n=5 separate adult samples, each experiment was run in triplicate, $P<0.05$). A panel of 3 reference genes was used to normalize the data.

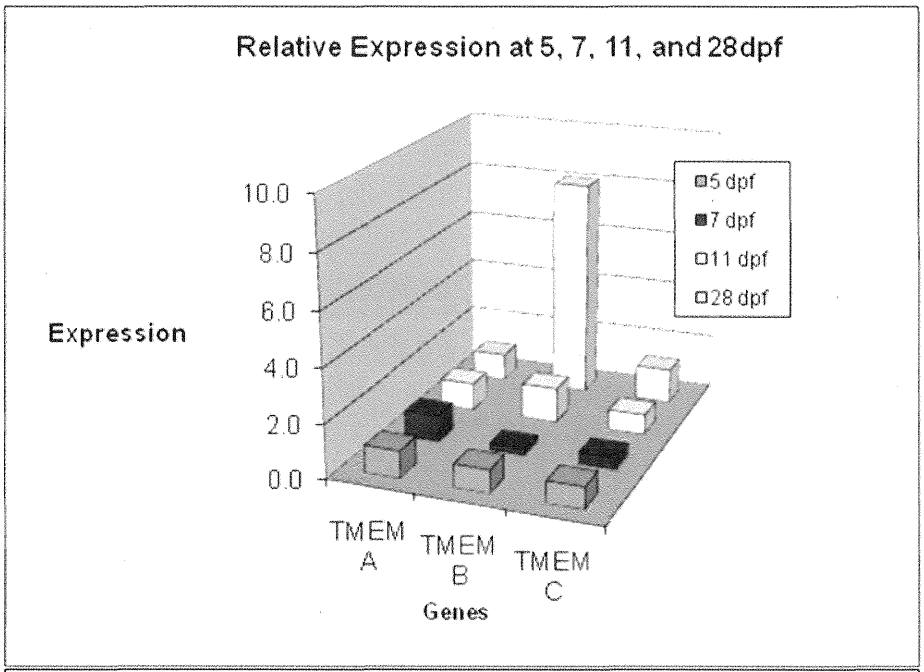

Figure 4. qPCR examining relative expression levels at specific developmental time points. Data are normalized to TMEMA expression at each timepoint.

Anti-anoctamin 1 antibodies were used to examine protein expression in zebrafish GI tissues. Zebrafish-specific antibodies are not available and anti-human and anti-mouse antibodies that have been shown to specifically identify anoctamin 1 were used[12]. ICC networks were identified in adult zebrafish GI tissues using a rabbit polyclonal antibody directed against a synthetic peptide of human anoctamin 1 (figure 6). Stellate-shaped ICC forming a dense network were observed in the myenteric plexus layer, located between the circular and smooth muscle layers. A second, less dense network of bipolar ICC was identified close to the Submucosal border. The immunostaining pattern is similar to that observed using anti-Kit antibody, and is similar to ICC observed in human and mouse small intestine[35]. These data suggest that anoctamin 1 is specifically expressed in zebrafish ICC and that anti-anoctamin 1 antibody selectively identifies ICC in the zebrafish.

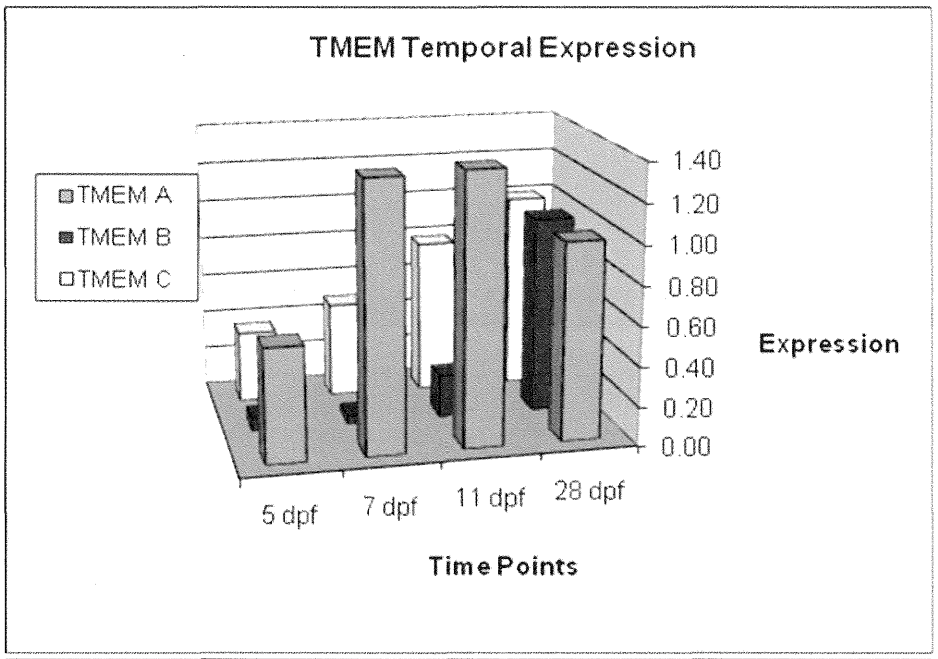

Figure 5. qPCR examining temporal expression patterns for TMEM16A, B, and C in isolated GI tissue. Timepoints shown are relative to expression level at 28 dpf.

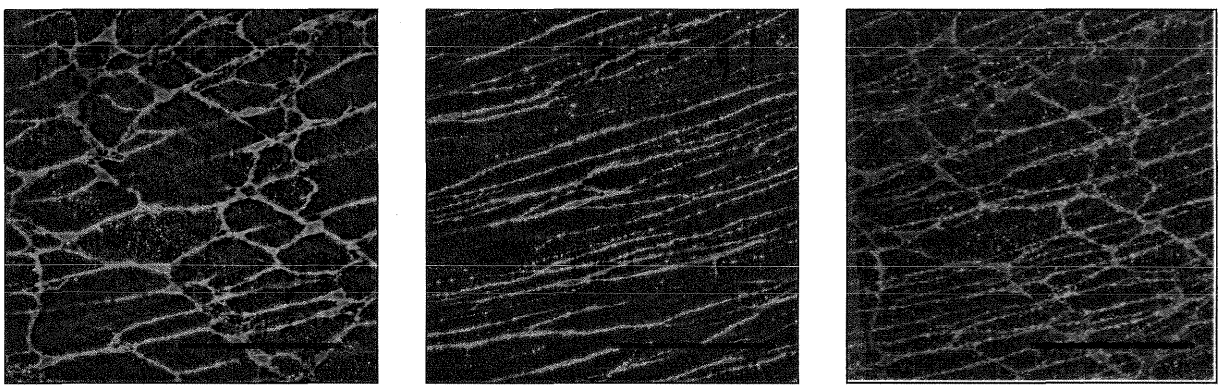

Figure 6. Anti-anoctamin 1 rabbit polyclonal antibody identifies ICC networks in adult zebrafish GI tract. Confocal stack reconstruction of 3 adjacent slices shows a high density of star-shaped myenteric ICC (left panel) located between the circular and longitudinal muscle layers, and bipolar ICC located near the submucosal border (middle panel). The right panel shows a full-thickness reconstruction containing myenteric and submucosal ICC networks. The scale bar is 100 μm.

Discussion

This study shows that anoctamin 1, 2, and 3 are expressed in GI tissues and that anoctamin 1 antibody identifies zebrafish ICC. Anoctamin 1 is a calcium activated chloride channel and contributes functionally to the development of the electrical slow wave by ICC in the mouse (Hwang et al, 2009). Transcription of anoctamin 1, 2, and 3 is also observed in epithelial layers in the developing mouse GI tract[13]. Our data suggest that anoctamin 1 is selectively expressed by zebrafish ICC, and no immunohistochemical staining was observed in the epithelial layers. More experiments are needed to verify this work, and to determine if epithelial expression of anoctamin 1, 2, and 3 occurs in the zebrafish GI tract. Specific antibodies to zebrafish proteins are relatively uncommon and therefore in-situ hybridization techniques are necessary.

The relative expression levels and temporal expression patterns were difficult to interpret. ICC are first observed at 7 dpf using anti-kit antibody[35]. q-PCR experiments show that the relative expression of anoctamin 2 is dominant in adult zebrafish, and that this pattern is evident by 28 dpf. There is some evidence in the literature that anoctamin 2 may be selectively expressed and functionally important in neural function. Transcription of anoctamin 2 was observed in dorsal root ganglion cells and in the neural tube, but was not evident in epithelial or in mesenchymal tissues in the mouse[13]. Anoctamin 2 is selectively expressed by olfactory sensory neurons in mice, and is functionally important for neural signaling there[33]. Anoctamin 2 is also expressed and is functionally relevant, in photoreceptor terminals[39]. Localization of transcription of anoctamin 2 will contribute to a better understanding for the functional role for anoctamin 2 in the zebrafish GI tract.

If anoctamin 1 is specifically expressed by ICC then expression would be expected to correlate with ICC development and ICC density. ICC are thought to begin to develop between 4 and 5 dpf, and full ICC networks are expected by 7 dpf. Thereafter ICC are anticipated to populate the GI tract and to increase in number as the GI tract grows, but density is expected to be relatively constant. It would be interesting to specifically lesion the ICC population using Gleevec®, a tyrosine kinase inhibitor, to see if anoctamin expression declines. It is essential to determine if GI epithelial cells express anoctamin 1, 2, and 3 to better understand the expression patterns and the role of these genes in GI function.

Future experiments should examine the role of anoctamin proteins on GI tract function. Pharmacological blockers of anoctamin 1, such as niflumic acid, may be

applied to zebrafish larvae and GI motility can be quantified[48]. These experiments will help to understand the functional role of anoctamin 1 on GI motility.

Kit/Kit Ligand

Background

The essential role of the receptor tyrosine kinase, Kit was identified from a spontaneous mouse mutant called White Spotting which showed that Kit is necessary for the development of melanocytes, germ cells, and hematopoietic stem cells[25]. Homozygous white spotting mice do not survive because of a lack of red blood cells[1]. Heterozygous white spotting mice survive to adulthood but kit activity is reduced by 90%. These mice weigh about 10% less compared to wildtype littermates, have gastrointestinal dysmotility, and lack ICC[1]. ICC populations can be lesioned by pharmacological inhibition of kit activity. Gleevec® is a kit receptor antagonist which received approval for the treatment of patients with KIT (CD117)-positive unresectable and/or metastatic malignant gastrointestinal stromal tumors (GIST) in 2002[30]. GIST is a cancer of the muscular wall of the GI tract which often involves over expression of the Kit receptor which leads to uncontrolled cell growth in ICC, forming a tumor. Treatment of GIST with Gleevec® decreases Kit activity, stops tumor growth, and shrinks tumors. Gleevec® administration to the mouse model results in the disappearance of ICC in adult mice or the ICC fail to develop in newborn mice[2]. Activating mutations in the KIT gene result in continuous or uncontrolled activation of the Kit receptor therefore, an excessive ICC growth and GIST development occur. Conversely, mutations that inactivate the Kit receptor or inhibiting Kit function pharmacologically, decreases ICC density. This is consistent with the essential role for Kit function in ICC development, growth, and maintenance. Other human GI motility disorders not involving mutations in the KIT gene result in a lack of or diminished population of ICC. Clinical symptoms of constipation, IBS, and gastroparesis, are caused by uncoordinated motility patterns which result from the lack of ICC pace-making ability.

Kit receptor is located in the plasma membrane of hematopoietic stem cells and ICC[18, 27]. It is activated when kit ligand binds, resulting in cell development and growth, and also plays an essential role on ICC survival[2]. Tyrosine kinase receptors, like Kit, have three functional domains; the extracellular ligand binding domain, the transmembrane domain, and the intracellular kinase domain. Ligand binding to extracellular domain results in dimerization of the receptor promoting auto-phosphorylation, and triggering enzymatic kinase activity. An intracellular enzymatic cascade results, and leads to cell growth. Ligand uncoupling removes the activating stimulus and turns Kit off.

Oncogenic activity of Kit was first discovered in the cat after isolation of a feline retrovirus from a fibrosarcoma[3]. The role of Kit in red blood cell development and as an oncogene has been widely examined. Expression of Kit on ICC in the GI tract was first discovered by Maeda and coworkers while examining Kit function during development[25]. Blocking Kit function with injection of a neutralizing antibody resulted in gross distension of the proximal small intestine in the BalbC strain of mice[25]. It is interesting that injection of the neutralizing antibody had no effect on the GI tract in several other strains of mice, including C57BL/6, C3H/He, CBA, and DBA/2 mice[25]. In summary, functional Kit activity is necessary for ICC development, growth and maintenance.

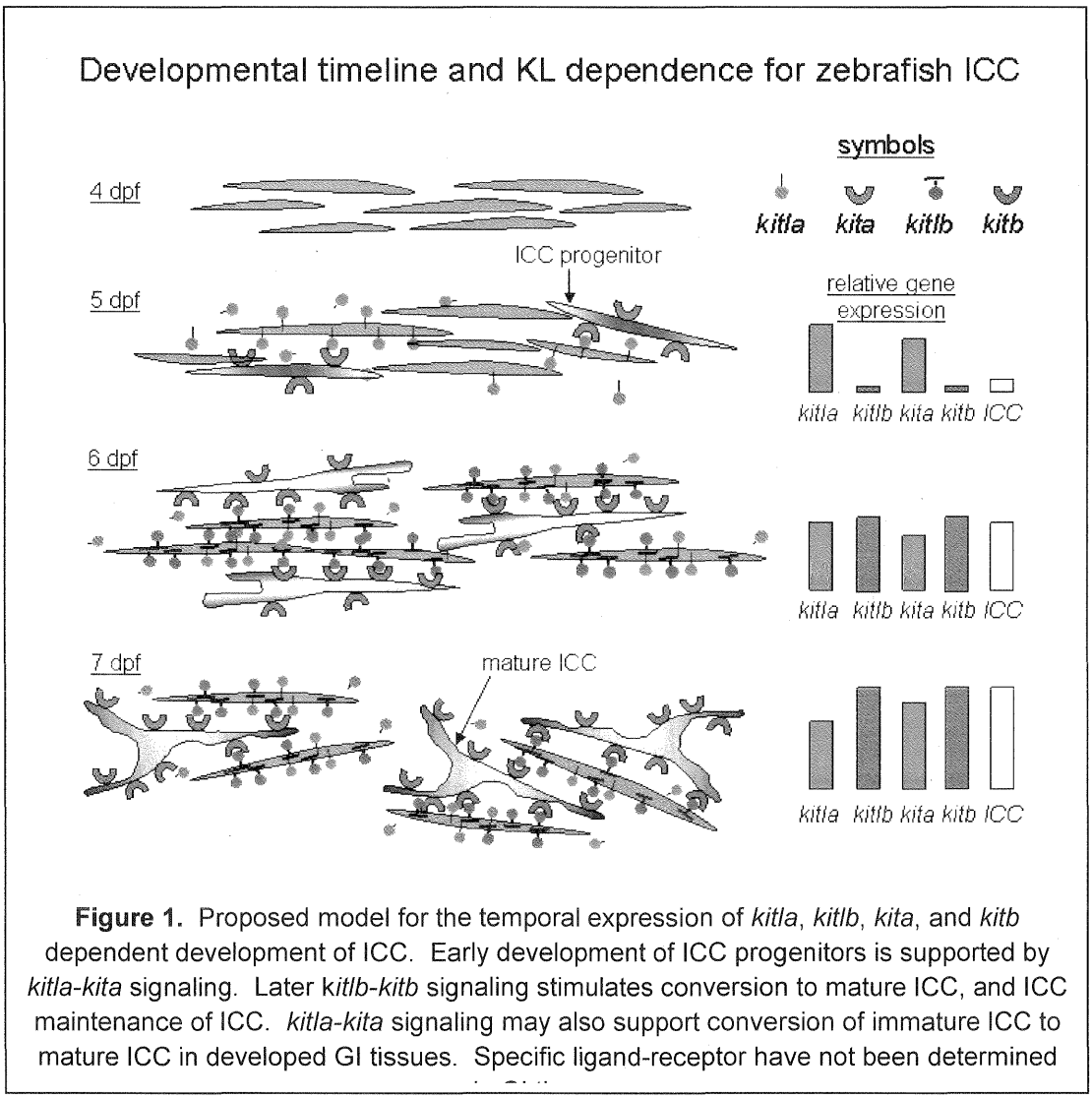

Figure 1. Proposed model for the temporal expression of *kitla*, *kitlb*, *kita*, and *kitb* dependent development of ICC. Early development of ICC progenitors is supported by *kitla-kita* signaling. Later k*itlb-kitb* signaling stimulates conversion to mature ICC, and ICC maintenance of ICC. *kitla-kita* signaling may also support conversion of immature ICC to mature ICC in developed GI tissues. Specific ligand-receptor have not been determined

The zebrafish expresses two orthologues to human Kit ligand, Kit ligand a and Kit ligand b (kitla and kitlb)[19]. Kit ligand is also called steel factor (SF), and stem cell factor in both humans and mice. For this thesis I will use SF to refer to human or mouse Kit ligand, and Kitla and Kitlb for zebrafish. Binding of SF to kit activates kit and is necessary for ICC development[36]. Spontaneous mutations in the mouse at the SF locus results in pigment defects, disrupted ICC networks, and GI motility defects, similar to mutations at the Kit locus[36]. Two isoforms of SF are expressed in humans and mouse, resulting in soluble SF and membrane-bound SF[36]. Membrane bound SF increases expression of ICC in culture, and soluble SF does not[36]. The role of soluble SF in ICC development is unknown. Recent work has shown the soluble SF may influence development and the maintenance of ICC progenitor cells located in the mouse GI tract[16].

One zebrafish orthologue, Kitla, corresponds to soluble SF and Kitlb corresponds to membrane-bound SF[19]. In the zebrafish model system morpholino (MO) knockdown experiments showed that Kitla plays an essential role in melanocyte migration, but Kitlb does not. A functional interaction between Kita and Kitla was verified using a temperature sensitive Kita mutant combined with MO knockdown of Kitla. The authors showed that a permissive temperature for the Kita mutant, allowing partial Kita function, was hypersensitive to a submaximal dose of Kitla MO[19]. The possible functional interaction between Kitb and Kitla or Kitlb remains. It is also possible that functional Kit-Kit ligand interactions differ in ICC compared to melanocytes.

This thesis is the first step in determining the role of Kita, Kitb, Kitla, and Kitlb in ICC development. At the mRNA level Kit ligand expression precedes Kit expression in the mouse[36]. We predict that functional receptor-ligand pairs will show this relationship in the zebrafish model system. A hypothetical relationship between Kitla - Kita, and Kitlb - Kitb is shown in Figure 1. This relationship was based on the idea that soluble Kit ligand supports development of ICC progenitors and that membrane-bound ligand supports ICC growth and maintenance. Smooth muscle populates the digestive tube early in development, and this is shown at 4 dpf. At 5 dpf expression of Kit ligand and Kit begins, and this supports development of ICC progenitors which convert to ICC later, near 6 dpf. We propose that Kitla (soluble) stimulates Kita early in development, near 5 dpf, supporting ICC differentiation and development from precursor cells. At 6 dpf Kitlb (membrane-bound) expression increases, and stimulates Kitb, supporting a conversion from ICC progenitor cells to ICC. This process continues at 7 dpf and is supported by Kitlb. For each functional

ligand-receptor pair we predict that the ligand mRNA expression will precede receptor mRNA expression.

Results/Discussion

Messenger RNA (mRNA) expression was measured using quantitative PCR techniques (qPCR) on cDNA prepared from total RNA that was isolated from GI tissue. GI tissues were dissected from zebrafish larvae at 5, 7, 11 dpf, from fully developed fish at 28 dpf, and from adults that were between 6 and 12 months old. All qPCR data was normalized to reference gene expression in the sample. Three reference genes were selected from a panel of reference genes verified to be appropriate for time course and tissue studies in the zebrafish model[41]. Reference gene expression was validated in our system based on the theory that expression of an ideal reference gene is not sensitive to experimental conditions. In this case, the experimental condition was development time point. Each reference gene appeared to change with developmental time point and therefore a panel of three reference genes was used.

We measured expression of Kita, Kitb, Kitla, and Kitlb, our genes of interest. We also measured the temporal expression pattern of SM-22, a gene that is expressed in all types of muscle cells during development and also in fully differentiated smooth muscle cells[23]. The GI tract grows substantially during the developmental time points that we selected and it is necessary to distinguish increased gene expression because of an increased number and size of the cells from a relative increase in gene expression. For example, a larger GI tract will have more smooth muscle cells, and more ICC. We would expect to see an increased amount of kita mRNA from these samples because there are more ICC expressing kita. We also expect to see more reference gene mRNA, because there are more cells expressing reference genes. When expression of kita is normalized to the reference gene expression we would not expect to see an increase in kita expression due to an increase in GI tract size. However, if expression of kita mRNA increases in individual ICC then relative expression will increase (compared to reference genes). We predicted that SM22 expression would increase with development as smooth muscle cells increase in number and in size.

Temporal expression was determined by normalizing raw Cq data to the average reference gene Cq for every time point. Normalized data was reported as relative to adult sample Cq data (formulas are given in experimental procedures). Figure 2 shows the temporal expression of Kita, Kitb, Kitla, Kitlb and SM-22. SM-22 expression increases steadily over time as expected because the smooth muscle in the gut is getting bigger. Kitlb expression is higher compared to Kitla expression at all time points. Expression of Kitlb and Kitla peaks at 11 dpf. Expression of Kita follows a similar pattern as Kitla, peaking at 11 dpf. Expression of Kitb follows a similar pattern as Kitlb, decreasing between 5 and 7 dpf, increasing at 11 dpf, and decreasing at 28 dpf. The data are consistent with functional pairs Kitb and Kitlb

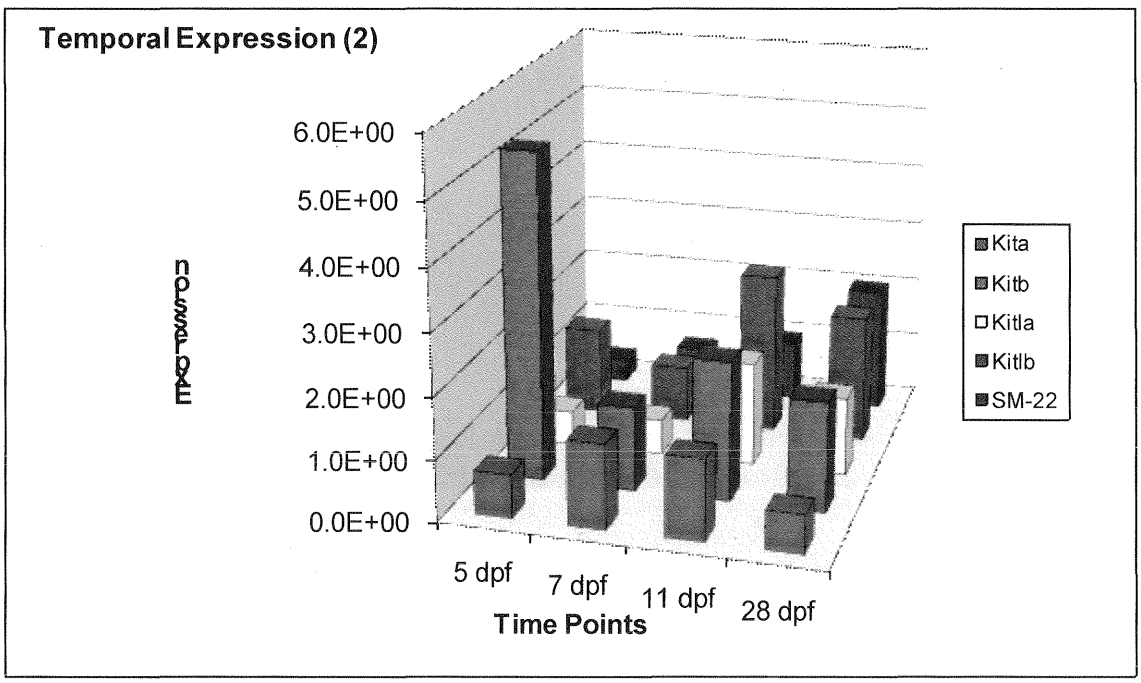

Figure 2. Temporal expression patterns of kita, kitb, kitla, and kitlb from total RNA isolated from zebrafish GI tissue at the indicated developmental time points. Expression data were normalized to a panel of reference genes, and are relative to adult expression levels.

because the expression patterns match. Kitlb may therefore influence conversion of ICC progenitors to mature ICC.

Relative expression determines the expression levels of all genes of interest at a single time point. This method of analysis gives a snapshot of expression at single time points, in contrast to temporal expression which shows how expression for each gene changes over time. Relative expression is determined by normalizing the raw Cq data to the average reference Cq for that gene at the same time point. The normalized data is compared to SM-22 expression at the same time point. The GI tract is

comprised of multiple layers of tissue, and includes a mucosal layer, circular and longitudional smooth muscle layers, and much smaller populations of regulatory cells such as enteric neurons and ICC. We do not know if the development of these subpopulations of cell types proceeds at similar rates. Therefore we used the smooth muscle marker, SM22, as a normalizing gene in relative expression so the growth of the GI tract would not influence data at the time point of interest. Figure 3 shows the relative expression at 5dpf, 7dpf, 11dpf, and 28dpf for Kita, Kitb, Kitla, and Kitlb.

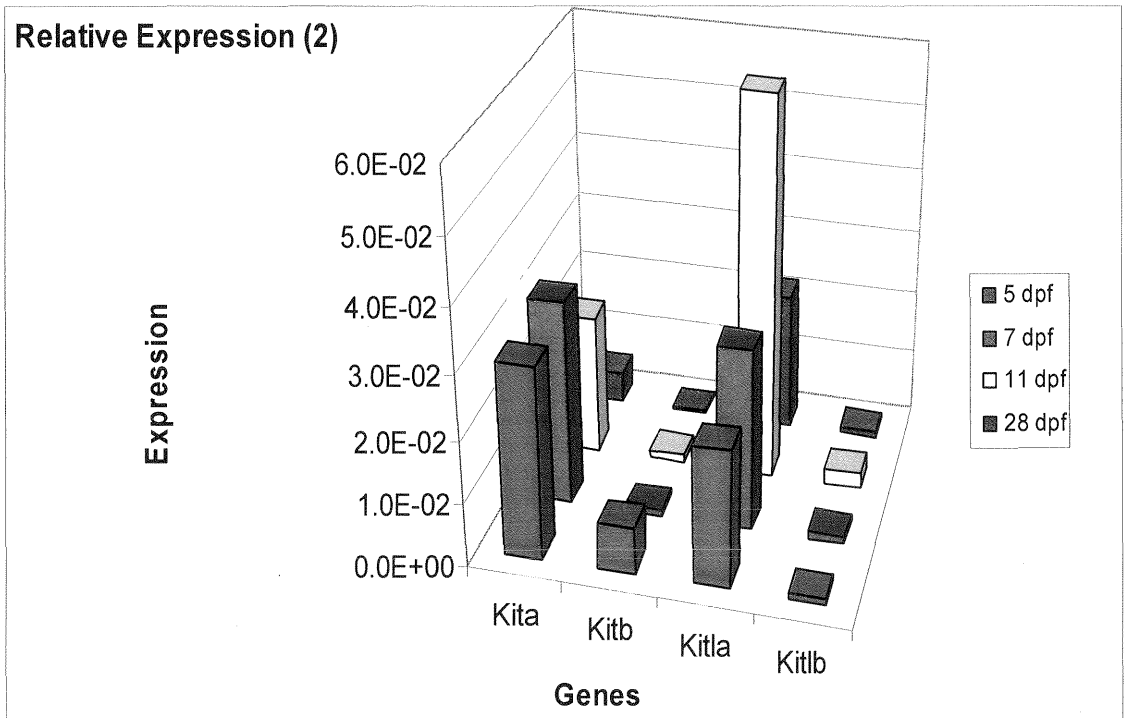

Figure 3: The relative expression at developmental and adult time points in the zebrafish GI tract of Kita, Kitb, Kitla, and Kitlb. Expression data was normalized to a panel of reference genes and is relative to SM-22 expression at the same time point.

Expression of Kita is higher compared to Kitb at each time point, and Kitla is higher compared to Kitlb at each time point. This suggests that Kita and Kitla are functional pairs, consistent with the role of Kitla activating Kita in melanocyte migration[19]. Similarly, the data are consistent with Kitb and Kitlb functional pairs.

Conclusion

The purpose of these experiments was to measure the relative and temporal expression of Kita, Kitb, Kitla, and Kitlb in the zebrafish gastrointestinal (GI) tract. Determining the expression levels of these genes involved in interstitial cells of Cajal (ICC) development, maintenance, and growth begins to explain the interactions and functions that these genes play in the GI tract. Real-time PCR was used to measure the expression levels. Real-time proved to be a sensitive technique with many potential pitfalls. In order to avoid some common error, such as RNA isolation/quality, pippetting technique, and lack of a single acceptable reference gene, great care was taken to keep data as honest as possible. These choices in protocol and analysis help to prevent overstated changes in expression but it is possible that true changes in expression levels over development are missed. Confidence in the data reported in this thesis is high; however conclusions contribute less to the ICC/GI story than expected. Further experiments are needed to confirm the data in this thesis. Protein expression is unknown; these data assume that RNA is translated into protein, so that more RNA means more functional protein. This is not necessarily true; there are other destinations for RNA such as degradation for regulatory processes. Localization of RNA is needed to ensure that expression measured is from ICC alone and not other cells within the GI tract. In situ hybridization experiments would provide this information.

References

1. Baxter, L. Hou, L. Loftus, S. Paven, K. (2004) Spotlight on Spotted Mice: A Review of White Spotting Mouse Mutants and Associated Human Pigmentation Disorders. *Pigment Cell Research* Volume 17, Issue 3, pages 215–224.
2. Beckett, E. Seungil, R. Bayquinov, Y. Sanders, K. Ward, S. (2007) Kit signaling is essential for development and maintenance of interstitial cells of Cajal and electrical rhythmicity in the embryonic gastrointestinal tract. *Dev Dyn* 236:60-72.
3. Besmer, P. Murphy, JE. George, PC. Qui, FH. Bergold, PJ. Lederman, L. Snyder, HW.
4. Brodeur, D. Zuckerman, EE. (1986) A new acute transforming feline retrovirus and relationship of its oncogene v-kit with the protein kinase gene family. *Nature* Apr 3-9; 320(6061): 415-21.
5. BIORAD Real-Time PCR Applications Guide.
6. Burns, AJ. (2007) Disorders of interstitial cells of Cajal. *J Pediatr Gastroenterol Nutr.* 45 Suppl 2:S103-6
7. Bustin, Stephen A. Benes, Vladimir. Garson, Jeremy A. Hellemans, Jan. Huggett, Jim. Kubista, Mikael. Mueller, Reinhold. Nolan, Tania. Pfaffl, Michael W. Shipley, Gregory L. Vandesompele, Jo. Wittwer, Carl T. (2009) The MIQE guidelines: Minimum information for publication of quantitative real-time PCR experiments. *Clinical Chemistry* 55(4): 611-622
8. Bustin, Stephen A. Nolan, Tania. (2004) Pitfalls of Quantitative Real-Time Reverse-Transcription Polymerase Chain Reaction. *Journal of Biomolecular Techniques* 15 (3): 155-166
9. Chen H, Ordög T, Chen J, Young DL, Bardsley MR, Redelman D, Ward SM, Sanders KM. (2007) Differential gene expression in functional classes of interstitial cells of Cajal in murine small intestine. *Physiol Genomics* 31(3): 492-509.
10. Espinosa I, Lee CH, Kim MK, Rouse BT, Subramanian S, Montgomery K, Varma S, Corless CL, Heinrich MC, Smith KS, Wang Z, Rubin B, Nielsen TO, Seitz RS, Ross DT, West RB, Cleary ML, van de Rijn M. (2008) A novel monoclonal antibody against DOG1 is a sensitive and specific marker for gastrointestinal stromal tumors. *Am J Surg Pathol* 32(2): 210-8.
11. Glenn, Sean. Jones, Craig. Liang, Ping. Kaushik, Dharam. Gross, Kenneth. Kim, Hyung. (2007) Expression profiling of archival renal tumors by quantitative PCR to validate prognostic markers. *BioTechniques* 43: 639-649
12. Gomez-Pinilla, Pedro J. Gibbons, Simon J. Bardsley, Michael R. Lorincz, Andrea. Pozo, Maria J. Pasricha, Pankaj J. Van de Rijn, Matt. West, Robert B. Sarr, Michael G. Kendrick, Michael L. Cima, Robert R. Dozois, Eric J. Larson, David W. Ordog, Tamas. Farrugia, Gianrico. (2009) Ano1 is a selective marker of interstitial cells of Cajal in the human and mouse

gastrointestinal tract. *Am J Physiol Gastrointest Liver Physiol* 296: G1370 – G1381
13. Gritli-Linde A, Vaziri Sani F, Rock JR, Hallberg K, Iribarne D, Harfe BD, Linde A. (2009) Expression patterns of the Tmem16 gene family during cephalic development in the mouse. *Gene Expr Patterns* 9(3): 178-91.
14. Holmberg A, Olsson C, Hennig GW. (2007) TTX-sensitive and TTX-insensitive control of spontaneous gut motility in the developing zebrafish (Danio rerio) larvae. *J Exp Biol* 210(6): 1084-91.
15. Hongbao Ma. Kuan-Jiunn Shieh. Geroge Chen. X. Tracy Qiao. Mei-Ying Chuang. (2006) Application of Real-Time Polymerase Chain Reaction (RT-PCR). *The Journal of American Science* 2(3):1-15
16. Horváth VJ, Vittal H, Lörincz A, Chen H, Almeida-Porada G, Redelman D, Ordög T. (2006) Reduced stem cell factor links smooth myopathy and loss of interstitial cells of cajal in murine diabetic gastroparesis. *Gastroenerology* 130(3):759-70
17. Huang, Fen. Rock, Jason R. Harfe, Brian D. Cheng, Tong. Huang, Xiaozhu. Jan, Yuh Nung. Jan, Lily Yeh. (2009) Studies on expression and function of the TMEM16A calcium-activated chloride channel. *PNAS* 106.50: 21413 – 21418
18. Huizinga, JD. Thuneburg, L. Kluppel, M. Mikkelsen, HB. Bernstein, A. (1995) W/kit gene required for interstitial cells of Cajal and for intestinal pacemaker activity. *Nature* 373: 347-349
19. Hultman, K.A., Bahary, N., Zon, L.I., and Johnson, S.L. (2007) Gene duplication of the zebrafish kit ligand and partitioning of melanocytes development functions to kit ligand a. *PLoS Genet.* 3(1):e17
20. Hwang, Sung Jin. Blair, Peter J. A. Britton, Fiona C. O'Driscoll, Kate E. Hannig, Grant. Bayguinov, Yulia R. Rock, Jason R. Harfe, Brian D. Sanders, Kenton M. Ward, Sean M. (2009) Expression of anoctamin 1/TMEM16A by interstitial cells of Cajal is fundamental for slow wave activity in gastrointestinal muscles. *J Physiol* 587.20: 4887-4904
21. Katz, Steven. DeMatteo, Ronald. (2008) Gastrointestinal stromal tumors and leiomyosarcomas. *Journal of Surgical Oncology* 97(4): 350-359.
22. Kluppel, M. Huizinga, JD. Malysa, J. Bernstein, A. (1998) Developmental origin and kit-dependent development of the interstitial cells of Cajal in the mammalian small intestine. *Dev Dyn* 211: 60-71
23. Li, L. Miano, JM. Cserjesi, P. Olson, EN. (1996) SM22 alpha, a marker of adult smooth muscle, is expressed in multiple myoger lineages durning embryogenesis. *Circ Res* Feb: 78 (2) 188-95
24. Liegl B, Hornick JL, Corless CL, Fletcher CD. (2009) Monoclonal antibody DOG1.1 shows higher sensitivity than KIT in the diagnosis of gastrointestinal stromal tumors, including unusual subtypes. *Am J Surg Pathol* 33(3): 437-46.
25. Maeda H, Yamagata A, Nishikawa S, Yoshinaga K, Kobayashi S, Nishi K, Nishikawa S. (1992) Requirement of c-kit for development of intestinal pacemaker system. Development 116(2):369-75

26. Mazzone A, Bernard CE, Strege PR, Beyder A, Galietta LJ, Pasricha PJ, Rae JL, Parkman HP, Linden DR, Szurszewski JH, Ordög T, Gibbons SJ, Farrugia G. (2011) Altered expression of ano1 variants in human diabetic gastroparesis. *J Biol Chem* 286(15): 13393-403.
27. Metzger, Roman. Rolle, Udo. Fiegel, Henning C. Franke, Folker E. Muenstedt, Karsten. Till, Holger. (2008) C-kit receptor in the human vas deferens: distinction of mast cells, interstitial cells, and interepithelial cells. *Reproduction* 135: 377-384
28. Nakahara, M. Isozaki, K. Vanderwiden, JM. Takakura, R. Kinoshita, K. Miyagawa, J. Chen, H. Miyazaki, Y. Kiyohara, T. Shinomura, Y. Matsuzawa, Y. (2002) Deficiency of KIT-positive cells in the colon of patients with diabetes mellitus. *J Gastroenterol Hepatol* 17.6: 666-670
29. Nishida, Toshirou. Takahashi, Tsuyoshi. Miyazaki, Yasuaki. (2009) Gastrointestinal stromal tumor: a bridge between bench and bedside. *Gastric Cancer* 12: 175-188
30. Novartis Pharmaceuticals Corporation. What Is GLEEVEC® and What Are Its Indications and Usage? (2011) http://www.gleevec.com/health-care-professional/indication-and-usage.jsp?usertrack.filter_applied=true&NovaId=2935376878979020262. Accessed April 28, 2011.
31. Nusslein-Volhard, Christine. Dahm, Ralf. (2002) Zebrafish, A Practical Approach. Oxford University Press Inc., New York
32. Parkman, Henry P. Doma, Sivaprasad. (2006) Importance of Gastrointestinal Motility Disorders. *Practical Gastroenterology* September: 23-40
33. Rasche S, Toetter B, Adler J, Tschapek A, Doerner JF, Kurtenbach S, Hatt H, Meyer H, Warscheid B, Neuhaus EM. (2010) Tmem16b is specifically expressed in the cilia of olfactory sensory neurons. *Chem Senses* 35(3): 239-45.
34. Rawls, John F. Johnson, Stephen L. (2000) Zebrafish kit mutation reveals primary and secondary regulation of melanocytes development during fin stripe regeneration. *Development* 127: 3715-3724
35. Rich, A. Leddon, S.A. Hess, S.L. Gibbons, S.J. Miller, S. Xu, X. Farrugai, G. (2007) Kit-Like Immunoreactivity in the Zebrafish Gastrointestinal Tract Reveals Putative ICC. *Developmental Dynamics* 236: 903-911
36. Rich, A. Miller, S. Gibbons, S. Malysz, J. Szurszewski, J. Farrugia, G. (2002) Local presentation of Steel factor increases expression of c-kit immunoreactive interstitial cells of Cajal in culture. *Am J Physiol Gastrointest Liver Physiol* 284: G313-G320.
37. Sanders, Kenton M. Ward, Sean M. (2006) Interstitial cells of Cajal: a new perspective on smooth muscle function. *J Physiol* 576.3: 721-726
38. Shimojima, N. Nakaki, T. Morikawa, Y. Hoshino, K. Kitajima, M. (2005) Imatinib blocks spontaneous mechanical activities in the adult mouse small intestine: possible inhibition of c-Kit signaling. *Pharmacology* 74(2): 95-99

39. Stöhr H, Heisig JB, Benz PM, Schöberl S, Milenkovic VM, Strauss O, Aartsen WM, Wijnholds J, Weber BH, Schulz HL. (2009) TMEM16B, a novel protein with calcium-dependent chloride channel activity, associates with a presynaptic protein complex in photoreceptor terminals. *J Neurosci* 29(21): 6809-18.
40. Tander, Burak. Bicakci, Unal. Sullu, Yardanur. Rizalar, Riza. Ariturk, Ender. Bernay, Ferit. Kandemir, Bedri. (2010) Alterations of Cajal cells in patients with small bowel atresia. *Journal of Pediatric Surgery* 45: 724-728
41. Tang, M. Dodd, A. Lai, D. Warren C. McNabb, Love, D. (2007) Validation of Zebrafish (Danio rerio) Reference Genes for Quantitative Real-time RT-PCR Normalization. ABBS 39 (5): 384-390
42. Vandesompele, Jo. De Preter, Katleen. Pattyn, Filip. Poppe, Bruce. Van Roy, Nadine. De Paepe, Anne. Speleman, Frank. (2002) Accurate normalization of real-time quantitative RT-PCR data by geometric averaging of multiple internal control genes. *Genome Biology* 3(7): research0034.1-0034.11
43. Wallace, Kenneth N. Akhter, Shafinaz. Smith, Erin M. Lorent, Kristin. Pack, Michael. (2004) Intestinal growth and differentiation in zebrafish. *Mechanisms of Development* 122: 157-173
44. Ward, SM. Burns, AJ. Torihashi, S. Sanders KM. (1994) Mutation of the proto-oncogene c-kit blocks development of interstitial cells and electrical rhythmicity in murine intestine. *J Physiol* 480, 91-97
45. West RB, Corless CL, Chen X, Rubin BP, Subramanian S, Montgomery K, Zhu S, Ball CA, Nielsen TO, Patel R, Goldblum JR, Brown PO, Heinrich MC, van de Rijn M (2004) The novel marker, DOG1, is expressed ubiquitously in gastrointestinal stromal tumors irrespective of KIT or PDGFRA mutation status. *AM J Pathol* 165(1):107-13.
46. Westerfield, Monte. (1995) The Zebrafish Book, A guide for the Laboratory use of zebrafish(Danio rerio). University of Oregon Press, Eugene
47. Yang, Young Duk. Cho, Hawon. Koo, Jae Yeon. Tak, Min Ho. Cho, Yeongyo. Shim, Won-Sik. Park, Seung Pyo. Lee, Jesun. Lee, Byeongjun. Kim, Byung-Moon. Raouf, Ramin. Shin, Young Ki. Oh, Uhtaek. (2008) TMEM16A confers receptor-activated calcium-dependant chloride conductance. *Nature* 455: 1210- 1216
48. Zhu, Mei Hong. Kim, Tae Wan. Ro, Seungil. Yan, Wei. Ward, Sean M. Koh, Sang Don. Sanders, Kenton M. (2009) A Ca^{2+}-activated Cl^- conductance in interstitial cells of Cajal linked to slow wave currents and pacemaker activity. *J Physiol* 587.20 4905-4918

Appendix 1: Procedures and Protocols

Appendix 1.1 Breeding Fish: Groups/Larvae Care

Breed fish in the morning

1.) Set up breeding boxes with a 3 female to 2 male fish ratio.
2.) Leave fish for 30-45 minutes
3.) Check for embryos
4.) Put fish back on the system rack
5.) Pour embryos through filter to separate from system water
6.) Rinse with E3 egg water
7.) Rinse embryos into petri dishes with E3 egg water (~ 25 embryos/dish)
8.) Fill petri dish half way with E3

Day 0 (6-8 hours later)

1.) Bleach embryos (Protocol separate)

Day 1

1.) Dechorinate embryos
    a. Using dissecting microscope and two pairs of dissection forceps, free embryos from chorion
    b. Remove debris from petri dish with a transfer pipett
    c. Fill petri dish to half full with E2 egg water

Day 2

1.) Clean larvae by removing most of the egg water with a transfer pipett, try to remove any debris or growth.
2.) Fill petri dish to half full with E2 egg water

Day 5

1.) Feed larvae HO, instant baby brine shrimp, or paramecium (if available)
2.) Add larvae to the rack system in the fish room
    a. Use smallest screen in the back of tank
    b. Add ~ 1-2 inches of system water

Day 7

1.) Feed HO/brine shrimp
2.) Increase water to ~ ½ - ¾ of the tank full

Day 11

1.) Begin feeding dry feed/brine shrimp
2.) Larvae should have full water flow into tank (slower then adult water flow)

When fry are large enough, change to larger screen in the back of the tank, then no screen at all.

Appendix 1.2: Bleaching Embryos

Embryos should be bleached on day 1 of development as follows:

1. Prepare bleach solution.

-50 mL Egg Water (E2), 35 uL Bleach

-Label bottle with date prepared. Bleach solution can be kept for up to one week.

2. Soak embryos in Bleach Solution for exactly 5 minutes. Trying to bleach more than two lines at once will make it difficult to be consistent and accurate.

-Pour off original egg water and add bleach solution until petri dish is at least half filled.

-Gently swirl dish so that the embryos are evenly separated.

3. Rinse embryos in Egg Water for 5 minutes.

-Pour off bleach solution.

Be careful to remove all the bleach by using a pipette

-Add Egg Water until dish is at least half filled.

-Gently swirl dish so that embryos are evenly separated.

4. Repeat steps #2 and #3 so that embryos are bleached and rinsed a total of TWO times.

5. Rinse embryos two more times in Egg Water for 5 minutes.

6. Divide embryos into dishes of no more than 50 and manually dechorionate on day 1 or day 2 of development, as they can no longer free themselves.

Appendix 1.3: E2 Egg Water Directions

1.) Solutions needed
   a. E2 (20X) in 1L Type I Water
      i. 17.5g NaCl
      ii. 0.75g KCl
      iii. 2.4g $MgSO_4$
      iv. 0.41g KH_2PO_4
      v. 0.12g Na_2HPO_4
   b. 7.25g $CaCl_2$/100ml Type I Water (Autoclaved)
   c. 3g $NAHCO_3$/100ml Type I Water (Autoclaved)
2.) 1X E2
   a. Combine 50ml 20X E2 stock, 2ml CaCl2, and 2ml NaHCO3
   b. Bring to 1L with Type I Water
   c. Adjust pH to 7.2

Appendix 1.4: RNA Isolation (Qiagen Kit)

1. Sample may be stored in RNA*later* for up to 7 days at room temperature or 4 weeks when refrigerated, fresh adult samples should be placed in 100ul (larvae in 30ul) RNA*later* before step 2.
2. Place sample and RNA*later* in a clean petri dish, cut with a sharp/clean razor. (Adult ONLY, Larvae samples go to step 3)
3. Transfer sample to a mortar tube and grind with pestle.
4. Sample should be in ~ 100ul (Adult) or 30ul (larvae) of RNA*later*, add 300ul Buffer RTL (w/ beta mercaptoethanol)
5. Suck up and eject sample with 20G needle on a 1cc sterile syringe 5 times, after the fifth time eject the sample onto the Qiagen Shredder column. (Purple)
6. Spin shredder column 2 minutes at max speed.
7. Remove shredder column, spin flow through 3 minutes at max speed.
8. Remove supernatant from first tube with a p1000. (Don't touch the bottom!)
9. Transfer supernatant to gDNA column. (clear with purple band)
10. Spin gDNA column 30 seconds.
11. SAVE flow through.
12. Add 300ul of 70% EtOH to flow through. Mix with pipette.
13. Put sample on the RNeasy column. (Pink)
14. Spin 30 seconds at max speed
15. Discard flow through
16. Add 600ul of Buffer RW1 to RNeasy column, spin at max speed 30 seconds
17. Discard flow through
18. Add 500ul of Buffer RPE to RNeasy column, spin at max speed for 30 seconds.
19. Discard flowthough.
20. Repeat steps 16 & 17.

21. Spin RNeasy column at max speed for two minutes to remove excess ethanol from column.
22. Place RNeasy column into a NEW TUBE (collection tube), add 50ul (adult) or 30ul (larvae) of nuclease free water to the column and spin at max speed 1 minute.
23. Put on Ice immediately.
24. Measure Absorption.
    a. Open NanoDrop 2000 program
    b. Click on nucleic acid
    c. Click no to open previous file
    d. Make sure arm is down and click ok for wavelength varification
    e. Clean NanoDrop 2000, see protocol above instrument.
    f. Add 1ul of nuclease free water to sampling area, click Blank.
    g. Wipe sampling area with a kimwipe.
    h. Add 1ul of sample to sampling area, click Measure.
    i. Record the concentration (ng/ul)

Appendix 1.5: Cleaning and Testing NanoDrop

Cleaning NanoDrop

This procedure will remove traces of old samples that have dried onto the sampling area and could affect readings.

1. Place 2uL of 0.5M HCl on the sampling area
2. Hit the Measure button on the software program
3. Let the HCl sit on the sampling area for 2 minutes
4. Wipe sampling area with a Kimwipe
5. Place 2uL of H_2O on the sampling area
6. Hit the Measure button on the software program
7. Wipe sampling area with a Kimwipe

The NanoDrop can now be blanked for the sample being tested.

Testing NanoDrop

This procedure will show that the NanoDrop is reading properly

1. Place 1uL of H_2O on sampling area
2. Hit the Blank button on the software program
3. Wipe the sampling area with a Kimwipe
4. Place 1uL of a DNA Ladder (Dye Free) on the sampling area
5. Hit the Measure button on the software program

   If a good curve and ratio appear then the NanoDrop is working; Wipe with a kimwipe and Blank for the sample being tested.

   If the curve and/or ratio is poor; Call Fisher Scientific Tech Support (302-479-7707)

   The lab spoke with Rick (ext. 164) Feb 2010

Appendix 1.6: cDNA Synthesis

	1X
5X Synthesis Buffer	4ul
dNTP mix	2ul
RT enhancer	1ul
Oligo dt	1ul
Verso Enzyme	1ul
Template (Total RNA)	(20ng)
Water	To volume
Total Volume	20ul

To determine volume of RNA:

ul RNA = 20ng divided by concentration of RNA (ng/ul)

Thermocycler Protocol:

Cycle	Temperature C	Time
1	42	30 minutes
2	95	2 minutes
3	10	∞

Test cDNA

1. Run PCR reaction using BioMix Red and the three-step protocol
    a. Use primers that amplify a large product (> 500bp)
2. Electrophoreses products in 2% agarose gel at 50mv for 1 hour
3. Visualize gel with ethidum bromide and UV Light
    a. Bands in all lanes at expected size confirms cDNA quality

Appendix 1.7: SYBR PCR Protocol

Cycle	Step	Temperature C	Time
1	1	95	3 minutes
2	1	95	10 seconds
	2	60	30 seconds
3 (Melt Curve)	1	55-95	30 seconds each temp
4	1	10	∞

Temperature Gradient PCR Protocol

Cycle	Step	Temperature C	Time
1	1	95	3 minutes
2	1	95	10 seconds
	2 (Temp. Gradient)	54-64	30 seconds
3 (Melt Curve)	1	55-95	30 seconds each temp
4	1	10	∞

SYBR PCR Mix

	1X
iQ SYBR Green Supermix	12.5ul
Template	1ul
Forward/Reverse Primers (20uM)	1ul

Water	10.5ul
Total Volume	25ul

*Use master-mixes whenever possible to limit pippetting errors

Appendix 1.8: Making 1E9

1.) Run a 50ul standard PCR reaction with primers for the gene of interest.

a. Using Bioline BioMix Red

	1X	2X
BioMix Red	12.5 ul	25ul
Template (wt adult zf gut)	1ul	2ul
For/Rev Primer 20uM	1ul	2ul
Water	10.5	21ul
Total Volume	25ul	50ul

b. Run reaction with a three-step PCR protocol

Cycle	Step	Temperature C	Time
1	1	95	3 minutes
2 (35X)	1	95	30 seconds
	2	60	30 seconds
	3	72	30 seconds
3	1	72	7 minutes
	2	10	∞

2.) Purify PCR product using Qiagen PCR Purification Kit

* Make sure Buffer PE has ethanol added to it*
- If not, see Buffer PE bottle for ethanol volume

a.) Add 5 volumes of Buffer PB to 1 volume of PCR reaction, Mix
- ex. Add 250ul Buffer PB to 50ul of PCR reaction

b.) Place a MiniElute column in a provided 2ml collection tube in a suitable rack

c.)To bind DNA, apply the sample to the MiniElute column
- spin at maximum speed for 1 minute

d.)Discard flow-through. Place the MiniElute Column in the same tube

e.) To wash, add 750ul Buffer PE to the MiniElute Column
- spin at maximum speed for 1 minute

f.) Discard flow-through. Place MiniElute Column in same tube.
- spin at maximum speed for 1 minute

(Must discard flow-through or additional ethanol will not come off column)

g.)Place MiniElute Column in a clean 1.5ml microcentrifuge tube

h.)To elute DNA, add 10ul Buffer EB (10mM Tris-Cl, pH 8.5) OR water to the **CENTER** of the membrane, let column sit 1 minute

- spin at max speed for 1 minute

* Average elute volume is 9ul*

3.) Determine OD of sample at 260nm

a. Start Nanodrop program
    i. Select nucleotides
b. Add 1ul of Buffer EB (PCR purification kit) or water to sampling area
    i. Hit blank button on software program
c. When ready for sample, wipe blank off of sampling area with a kimwipe
d. Add 1ul of sample to sampling area
    i. Hit measure button on software program
e. Record A260 reading

4.) Use A260 reading to calculate concentration, then molecules/ul

a. Concentration (ug/ul)

    = A260 * Dilution Factor * Pathlength * 0.5ng/ul

b. Determine molecules/ul

    Concentration (ug/ul) * 0.0001 =

    Concentration (g/ul) * Average nucleotide molecular weight (630g/mol) = Concentration (mol of bp/ul) * 1/# of base pairs in the product =

    Concentration (mol of product/ul) * Avagadro's # (6.02×10^{23} molecules/mol)=

    Concentration (molecules/ul)

5.) Determine 1E9, make solution

C1 V1 = C2 V2

Where C1 = concentration (molecules/ul) of sample

C2 = concentration (1E9 molecules/ul)

V1= 2ul

V2= ul of water to add to 2ul of sample

6.) Dilute 1E9 for standard curve
   a. 1ul of 1E9 in 99ul of water gives 1E7
   b. 1ul of 1E7 in 9ul of water gives 1E6
   c. Continue 1:10 dilution to get 1E5 – 1E1

Appendix 1.9: Real-time PCR Experimental Outline

I. Optimize Primers (Use WT Adult Gut template)
   a. Temperature Gradient
      i. Single peak melt curve
      ii. Single band on agarose gel
      iii. Determine optimal temperature
   b. Standard Curve
      i. 1E7 to 1E1
      ii. Single peak on melt curve
      iii. Efficiency of 90-110%
         1. All primer sets have similar efficiencies (within 5%)
      iv. r > 0.980

II. Create samples
   a. Time points: 5, 7, 11, 24 dpf, Adult
   b. Samples for each time point
      i. Isolate RNA
      ii. Make cDNA
         1. Make 30ul aliquots to freeze

III. q-PCR Reactions
   a. Design plate
   b. Plan master mix
      i. 1X SYBR reaction in separate protocol
   c. Run PCR on MyiQ thermocycler

IV. Data Analysis

Appendix 1.10 Experimental Outline Summary

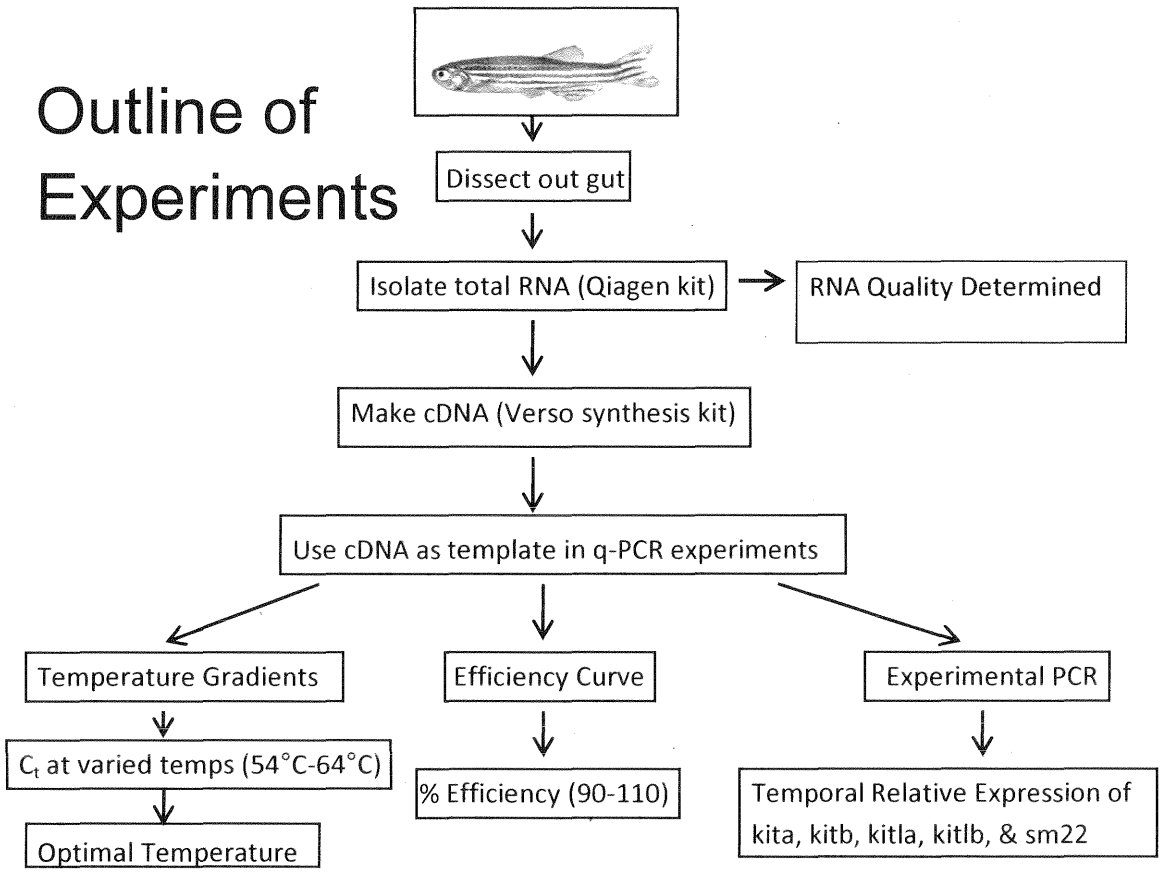

Appendix 2: Real-Time Data

Appendix 2.1: Experiment 1/Kita

Condition	Gene	Mean Cq	Ct SD	Avg. REF Cq	Delta Cq
5dpf	Kita	32.05	0.65		-11.06
5dpf	Bactin RT	20.88	0.11	20.99	
5dpf	EF1alpha	21.13	0.04		
5dpf	Rpl13alpha	20.97	0.05		
7dpf	Kita	31.27	0.42		-10.38
7dpf	Bactin RT	21.09	0.12	20.89	
7dpf	EF1alpha	20.75	0.04		
7dpf	Rpl13alpha	20.84	0.02		
11dpf	Kita	32.33	0.51		-9.13
11dpf	Bactin RT	23.28	0.06	23.20	
11dpf	EF1alpha	23.61	0.05		
11dpf	Rpl13alpha	22.71	0.03		
28dpf	Kita	33.70	0.64		-11.04
28dpf	Bactin RT	22.61	0.04	22.66	
28dpf	EF1alpha	22.33	0.08		
28dpf	Rpl13alpha	23.03	0.05		
Adult1	Kita	31.04	0.76		-10.50
Adult1	Bactin RT	19.83	0.04	20.54	
Adult1	EF1alpha	20.95	0.08		
Adult1	Rpl13alpha	20.85	0.02		
Adult2	Kita	29.56	0.60		-10.35
Adult2	Bactin RT	18.65	0.02	19.21	
Adult2	EF1alpha	18.96	0.01		
Adult2	Rpl13alpha	20.01	0.03	AVG	-10.41
				stdev	0.70
	Adult Averages				
	Kita	30.30			-10.43
	Bactin RT	19.24		19.88	
	EF1alpha	19.96			
	Rpl13alpha	20.43			

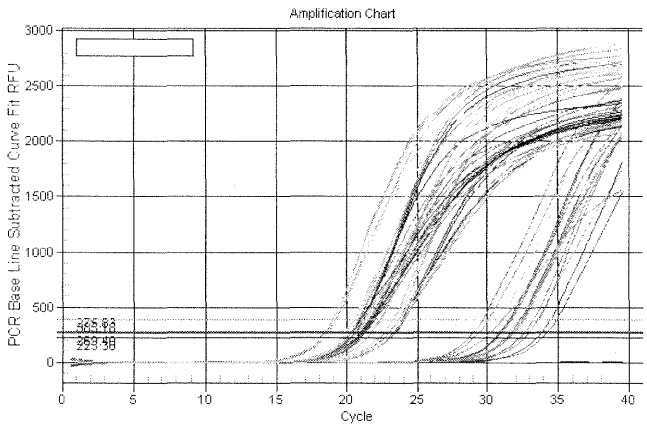

Appendix 2.2: Experiment 1/Kitb

Condition	Gene	Mean Cq	Cq SD	Avg. REF Cq	Delta Cq
5dpf	Kitb	35.58	0.712		-14.63
5dpf	Bactin RT	20.81	0.115	20.95	
5dpf	EF1alpha	21.03	0.143		
5dpf	Rpl13alpha	21.01	0.042		
7dpf	Kitb	36.08	0.855		-15.22
7dpf	Bactin RT	21.07	0.107	20.86	
7dpf	EF1alpha	20.66	0.021		
7dpf	Rpl13alpha	20.85	0.025		
11dpf	Kitb	34.34	1.517		-11.16
11dpf	Bactin RT	23.23	0.05	23.18	
11dpf	EF1alpha	23.59	0.021		
11dpf	Rpl13alpha	22.72	0.027		
28dpf	Kitb	32.4	0.86		-9.67
28dpf	Bactin RT	22.68	0.082	22.73	
28dpf	EF1alpha	22.41	0.04		
28dpf	Rpl13alpha	23.1	0.007		
Adult1	Kitb	32.49	0.644		-12.0267
Adult1	Bactin RT	19.77	0.059	20.463333	
Adult1	EF1alpha	20.72	0.025		
Adult1	Rpl13alpha	20.9	0.047		
Adult2	Kitb	29.01	0.182		-9.76333
Adult2	Bactin RT	18.69	0.009	19.246667	
Adult2	EF1alpha	19	0.061		
Adult2	Rpl13alpha	20.05	0.104	AVG	-12.0783
				stdev	2.382703
	Adult Averages				
	Kitb	30.75			-10.895
	Bactin RT	19.23		19.855	
	EF1alpha	19.86			
	Rpl13alpha	20.475			

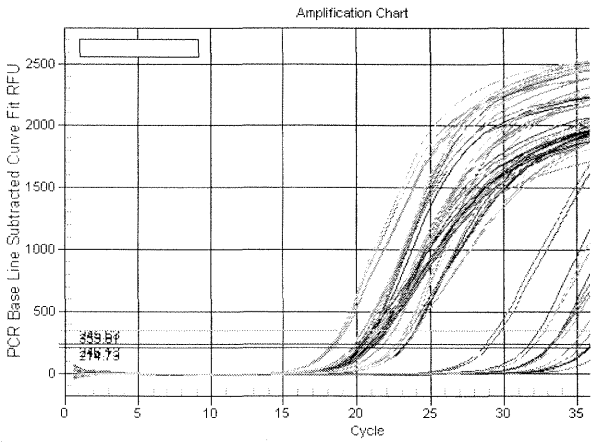

Appendix 2.3: Experiment 1/kitla

Condition	Gene	Mean Cq	Cq SD	Avg. Ref Cq	delta Cq
5dpf	Kitla	29.67	0.07		-8.8
5dpf	Bactin RT	20.75	0.13	20.87	
5dpf	EF1alpha	20.95	0.005		
5dpf	Rpl13alpha	20.91	0.046		
7dpf	Kitla	29.12	0.188		-8.35
7dpf	Bactin RT	21.04	0.119	20.77	
7dpf	EF1alpha	20.48	0.046		
7dpf	Rpl13alpha	20.79	0.038		
11dpf	Kitla	30.95	0.097		-7.93667
11dpf	Bactin RT	23.12	0.057	23.01333	
11dpf	EF1alpha	23.29	0.137		
11dpf	Rpl13alpha	22.63	0.04		
28dpf	Kitla	29.63	0.27		-7.01667
28dpf	Bactin RT	22.5	0.048	22.61333	
28dpf	EF1alpha	22.42	0.29		
28dpf	Rpl13alpha	22.92	0.022		
Adult1	Kitla	27.69	0.098		-7.29
Adult1	Bactin RT	19.71	0.033	20.4	
Adult1	EF1alpha	20.66	0.088		
Adult1	Rpl13alpha	20.83	0.033		
Adult2	Kitla	25.73	0.058		-6.64667
Adult2	Bactin RT	18.45	0.063	19.08333	
Adult2	EF1alpha	18.84	0.069		
Adult2	Rpl13alpha	19.96	0.016	AVG	-7.67333
				stdev	0.828106
	Adult Averages				
	Kitla	26.71			-6.96833
	Bactin RT	19.08		19.74167	
	EF1alpha	19.75			
	Rpl13alpha	20.395			

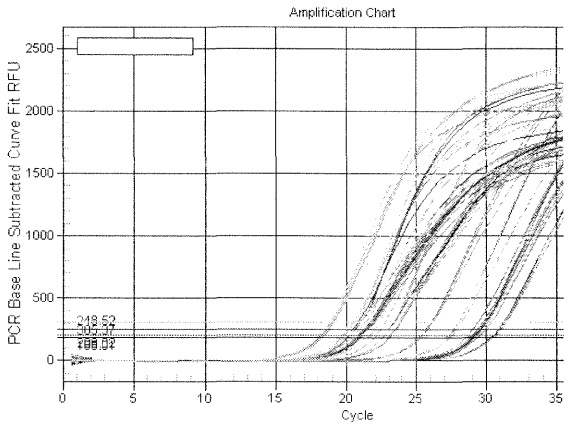

Appendix 2.4: Experiment 1/kitlb

Condition	Gene	Mean Cq	Cq SD	avg REF Cq	delta Cq
5dpf	Kitlb	25.33	0.477		-4.35
5dpf	Bactin RT	21.07	0.106	20.98	
5dpf	EF1alpha	20.71	0.174		
5dpf	Rpl13alpha	21.16	0.029		
7dpf	Kitlb	30.05	0.093		-9.04
7dpf	Bactin RT	21.15	0.114	21.01	
7dpf	EF1alpha	20.63	0.045		
7dpf	Rpl13alpha	21.25	0.051		
11dpf	Kitlb	32.3	0.252		-9.12
11dpf	Bactin RT	23.09	0.062	23.18	
11dpf	EF1alpha	23.72	0.047		
11dpf	Rpl13alpha	22.73	0.016		
28dpf	Kitlb	30.73	0.329		-7.80667
28dpf	Bactin RT	22.84	0.083	22.92333	
28dpf	EF1alpha	22.49	0.166		
28dpf	Rpl13alpha	23.44	0.034		
Adult1	Kitlb	29.65	0.07		-9.01667
Adult1	Bactin RT	20.36	0.512	20.63333	
Adult1	EF1alpha	20.57	0.071		
Adult1	Rpl13alpha	20.97	0.034		
Adult2	Kitlb	27.63	0.168		-8.18667
Adult2	Bactin RT	19.02	0.062	19.44333	
Adult2	EF1alpha	18.98	0.055		
Adult2	Rpl13alpha	20.33	0.012	AVG	-7.92
				stdev	1.828985
	Adult Averages				
	Kitlb	28.64			-8.60167
	Bactin RT	19.69		20.03833	
	EF1alpha	19.775			
	Rpl13alpha	20.65			

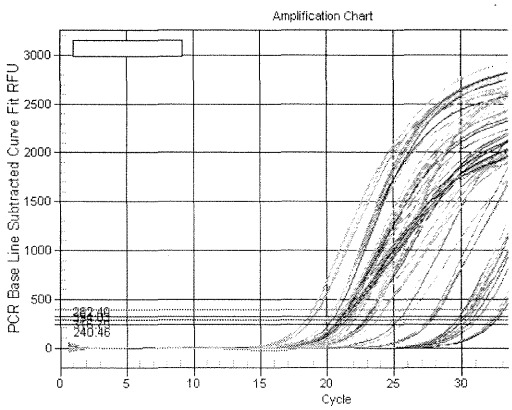

Appendix 2.5: Experiment 1/sm-22

Condition	Gene	Mean Cq	Cq SD	avg REF Cq	delta Cq
5dpf	SM-22	25.11	0.224		-4.38
5dpf	Bactin RT	20.52	0.129	20.73	
5dpf	EF1alpha	20.83	0.04		
5dpf	Rpl13alpha	20.84	0.031		
7dpf	Sm-22	24.6	0.23		-3.85667
7dpf	Bactin RT	20.99	0.099	20.74333	
7dpf	EF1alpha	20.51	0.075		
7dpf	Rpl13alpha	20.73	0.014		
11dpf	SM-22	26.3	0.331		-3.15
11dpf	Bactin RT	23.8	1.548	23.15	
11dpf	EF1alpha	23.24	0.624		
11dpf	Rpl13alpha	22.41	0.033		
28dpf	SM-22	27.04	0.186		-4.47333
28dpf	Bactin RT	22.49	0.175	22.56667	
28dpf	EF1alpha	22.3	0.05		
28dpf	Rpl13alpha	22.91	0.018		
Adult1	SM-22	25.6	0.188		-5.41333
Adult1	Bactin RT	19.65	0.018	20.18667	
Adult1	EF1alpha	20.1	0.123		
Adult1	Rpl13alpha	20.81	0.13		
Adult2	SM-22	25.1	0.134		-6.26
Adult2	Bactin RT	18.35	0.072	18.84	
Adult2	EF1alpha	18.45	0.01		
Adult2	Rpl13alpha	19.72	0.148	AVG	-4.58889
				stdev	1.107778
	Adult Averages				
	SM-22	25.35			-5.83667
	Bactin RT	19		19.51333	
	EF1alpha	19.275			
	Rpl13alpha	20.265			

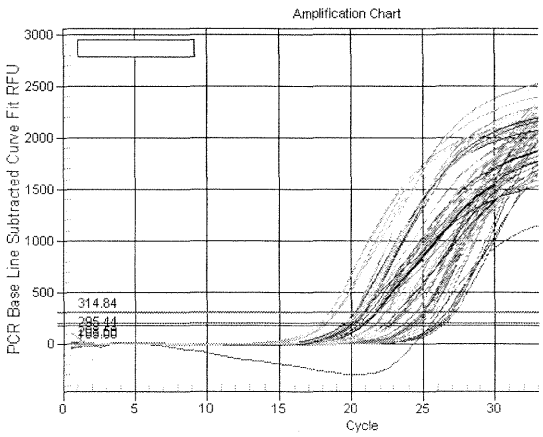

Appendix 2.6: Experiment 2/kita

Condition	Gene	Mean Cq	Cq SD	Avg. Ref Cq	delta Cq
5dpf	Kita	30.1	0.283		-10.4
5dpf	Bactin RT	19.48	0.132	19.7	
5dpf	EF1alpha	19.36	0.05		
5dpf	Rpl13alpha	20.26	0.046		
7dpf	Kita	29.07	0.147		-9.44
7dpf	Bactin RT	19.91	0.113	19.63	
7dpf	EF1alpha	19.26	0.066		
7dpf	Rpl13alpha	19.72	0.056		
11dpf	Kita	29.23	0.13		-9.5
11dpf	Bactin RT	19.5	0.46	19.73	
11dpf	EF1alpha	19.43	0.032		
11dpf	Rpl13alpha	20.26	0.024		
28dpf	Kita	31.6	0.248		-10.5667
28dpf	Bactin RT	20.37	0.023	21.03333	
28dpf	EF1alpha	20.95	0.066		
28dpf	Rpl13alpha	21.78	0.042		
Adult1	Kita	29.55	0.79		-9.69667
Adult1	Bactin RT	19.29	0.04	19.85333	
Adult1	EF1alpha	19.86	0.016		
Adult1	Rpl13alpha	20.41	0.037		
Adult2	Kita	31.2	0.17		-10.1133
Adult2	Bactin RT	19.85	0.072	21.08667	
Adult2	EF1alpha	20.81	0.49		
Adult2	Rpl13alpha	22.6	0.348	AVG	-9.95278
				stdev	0.476694
	Adult Averages				
	Kita	30.375			-9.905
	Bactin RT	19.57		20.47	
	EF1alpha	20.335			
	Rpl13alpha	21.505			

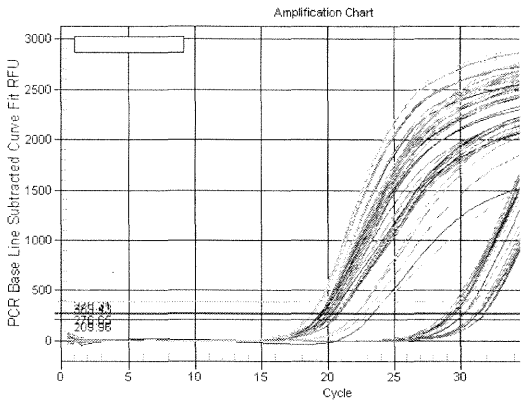

Appendix 2.7: Experiment 2/kitb

Condition	Gene	Mean Cq	Cq SD	Avg. Ref Cq	delta Cq
5dpf	Kitb	32.05	0.433		-12.4167
5dpf	Bactin RT	19.4	0.17	19.63333	
5dpf	EF1alpha	19.11	0.056		
5dpf	Rpl13alpha	20.39	0.043		
7dpf	Kitb	33.88	0.557		-14.3667
7dpf	Bactin RT	19.81	0.057	19.51333	
7dpf	EF1alpha	18.99	0.055		
7dpf	Rpl13alpha	19.74	0.047		
11dpf	Kitb	33.25	0.597		-13.6433
11dpf	Bactin RT	19.34	0.003	19.60667	
11dpf	EF1alpha	19.17	0.028		
11dpf	Rpl13alpha	20.31	0.076		
28dpf	Kitb	35	1.099		-13.9833
28dpf	Bactin RT	20.32	0.015	21.01667	
28dpf	EF1alpha	20.81	0.042		
28dpf	Rpl13alpha	21.92	0.082		
Adult1	Kitb	35.35	0.491		-15.5633
Adult1	Bactin RT	19.15	0.021	19.78667	
Adult1	EF1alpha	19.7	0.059		
Adult1	Rpl13alpha	20.51	0.035		
Adult2	Kitb	35.21	0.915		-14.0867
Adult2	Bactin RT	19.77	0.055	21.12333	
Adult2	EF1alpha	20.65	0.038		
Adult2	Rpl13alpha	22.95	0.494	AVG	-14.01
				stdev	1.021744
	Adult Averages				
	Kitb	35.28			-14.825
	Bactin RT	19.46		20.455	
	EF1alpha	20.175			
	Rpl13alpha	21.73			

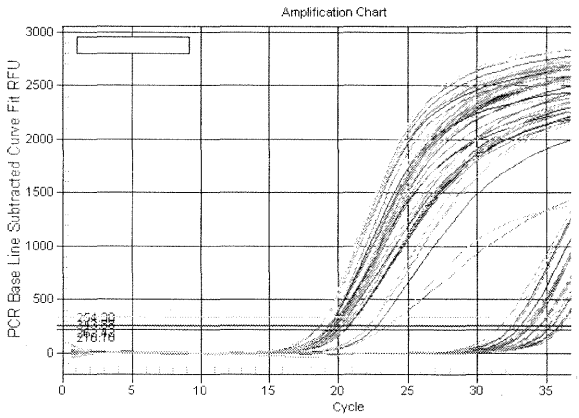

Appendix 2.8: Experiment 2/kitla

Condition	Gene	Mean Cq	Cq SD	Avg Ref Cq	delta Cq
5dpf	Kitla	29.34	0.066		-9.65
5dpf	Bactin RT	19.41	0.146	19.69	
5dpf	EF1alpha	19.26	0.037		
5dpf	Rpl13alpha	20.4	0.117		
7dpf	Kitla	29.21	0.216		-9.61
7dpf	Bactin RT	19.8	0.09	19.6	
7dpf	EF1alpha	19.18	0.015		
7dpf	Rpl13alpha	19.82	0.068		
11dpf	Kitla	27.75	0.134		-8.05667
11dpf	Bactin RT	19.41	0.05	19.69333	
11dpf	EF1alpha	19.34	0.031		
11dpf	Rpl13alpha	20.33	0.027		
28dpf	Kitla	29.54	0.179		-8.46667
28dpf	Bactin RT	20.3	0.048	21.07333	
28dpf	EF1alpha	20.95	0.052		
28dpf	Rpl13alpha	21.97	0.041		
Adult1	Kitla	28.63	0.32		-8.81333
Adult1	Bactin RT	19.15	0.068	19.81667	
Adult1	EF1alpha	19.79	0.046		
Adult1	Rpl13alpha	20.51	0.115		
Adult2	Kitla	29.85	0.29		-8.81333
Adult2	Bactin RT	19.87	0.116	21.03667	
Adult2	EF1alpha	20.72	0.046		
Adult2	Rpl13alpha	22.52	0.093	AVG	-8.90167
				stdev	0.62938
	Adult Averages				
	Kitla	29.24			-8.81333
	Bactin RT	19.51		20.42667	
	EF1alpha	20.255			
	Rpl13alpha	21.515			

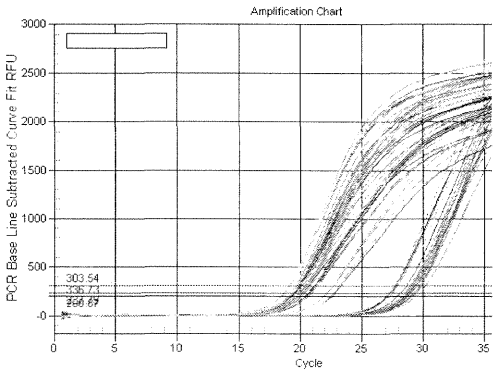

Appendix 2.9: Experiment 2/kitlb

Condition	Gene	Mean Cq	Cq SD	Avg. Ref Cq	delta Cq
5dpf	Kitlb	33.21	0.115		-13.4867
5dpf	Bactin RT	19.42	0.171	19.72333	
5dpf	EF1alpha	19.19	0.071		
5dpf	Rpl13alpha	20.56	0.119		
7dpf	Kitlb	33.76	0.94		-14.1367
7dpf	Bactin RT	19.89	0.052	19.62333	
7dpf	EF1alpha	19.1	0.066		
7dpf	Rpl13alpha	19.88	0.085		
11dpf	Kitlb	32.38	0.651		-12.6067
11dpf	Bactin RT	19.52	0.074	19.77333	
11dpf	EF1alpha	19.26	0.069		
11dpf	Rpl13alpha	20.54	0.092		
28dpf	Kitlb	34.06	0.152		-12.9533
28dpf	Bactin RT	20.45	0.021	21.10667	
28dpf	EF1alpha	20.9	0.057		
28dpf	Rpl13alpha	21.97	0.044		
Adult1	Kitlb	33.62	0.434		-13.6967
Adult1	Bactin RT	19.28	0.026	19.92333	
Adult1	EF1alpha	19.76	0.055		
Adult1	Rpl13alpha	20.73	0.06		
Adult2	Kitlb	35.43	1.543		-14.3167
Adult2	Bactin RT	19.9	0.031	21.11333	
Adult2	EF1alpha	20.72	0.072		
Adult2	Rpl13alpha	22.72	0.102	AVG	-13.5328
				stdev	0.663564
	Adult Averages				
	Kitlb	34.525			-14.0067
	Bactin RT	19.59		20.51833	
	EF1alpha	20.24			
	Rpl13alpha	21.725			

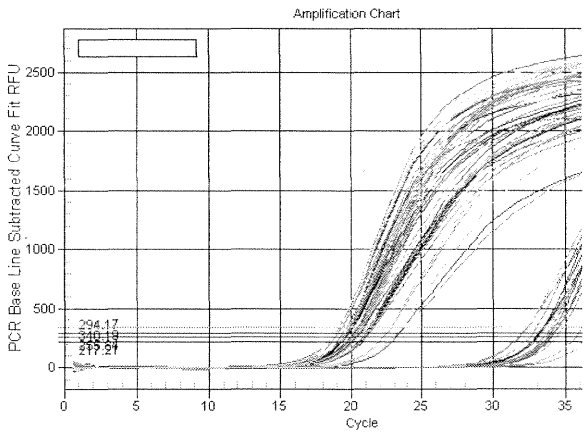

Appendix 2.10: Experiment 2/sm-22

Condition	Gene	Mean Cq	Cq SD	Avg Ref Cq	delta Cq
5dpf	SM-22	25	0.515		-5.34667
5dpf	Bactin RT	19.41	0.124	19.65333	
5dpf	EF1alpha	19.01	0.072		
5dpf	Rpl13alpha	20.54	0.027		
7dpf	Sm-22	24.1	0.083		-4.48
7dpf	Bactin RT	19.9	0.022	19.62	
7dpf	EF1alpha	19.03	0.076		
7dpf	Rpl13alpha	19.93	0.067		
11dpf	SM-22	23.7	0.149		-3.99333
11dpf	Bactin RT	19.5	0.036	19.70667	
11dpf	EF1alpha	19.12	0.044		
11dpf	Rpl13alpha	20.5	0.064		
28dpf	SM-22	24.02	0.121		-2.94
28dpf	Bactin RT	20.34	0.028	21.08	
28dpf	EF1alpha	20.82	0.076		
28dpf	Rpl13alpha	22.08	0.057		
Adult1	SM-22	24.43	0.205		-4.50667
Adult1	Bactin RT	19.33	0.24	19.92333	
Adult1	EF1alpha	19.68	0.058		
Adult1	Rpl13alpha	20.76	0.048		
Adult2	SM-22	24.51	0.102		-3.41667
Adult2	Bactin RT	19.88	0.14	21.09333	
Adult2	EF1alpha	20.66	0.064		
Adult2	Rpl13alpha	22.74	0.035	AVG	-4.11389
				stdev	0.858687
	Adult Averages				
	SM-22	24.47			-3.96167
	Bactin RT	19.605		20.50833	
	EF1alpha	20.17			
	Rpl13alpha	21.75			

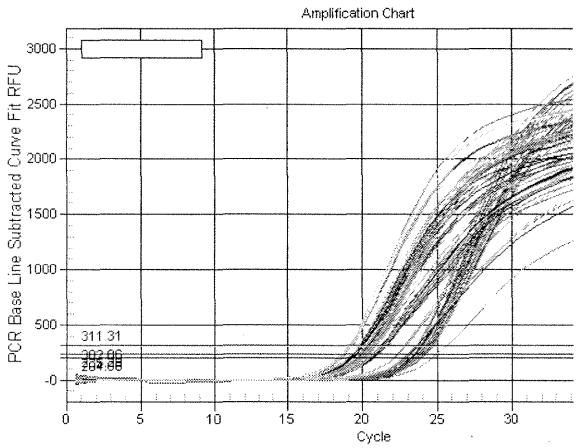

Appendix 2.11: Experiment 1 Summary

Relative to Adult Expression and Normalized to Reference Genes

temporal expression for individual genes	Kita					Kitb				
	Cq	Avg Ref Cq	delta Cq	NE	RE	Cq	Avg Ref Cq	delta Cq	NE	RE
5 dpf	32.05	20.99	-11.06	4.7E-04	0.65	35.58	20.95	-14.63	3.9E-05	0.08
7 dpf	31.27	20.89	-10.38	7.5E-04	1.03	36.08	20.86	-15.22	2.6E-05	0.05
11 dpf	32.33	23.20	-9.13	1.8E-03	2.45	34.34	23.18	-11.16	4.4E-04	0.83
28 dpf	33.70	22.66	-11.04	4.7E-04	0.65	32.40	22.73	-9.67	1.2E-03	2.34
adult (Calibrator)	30.30	19.88	-10.43	7.3E-04	1.00	30.75	19.86	-10.90	5.3E-04	1.00

temporal expression for individual genes	Kitla					Kitlb					Sm-22				
	Cq	Avg Ref Cq	delta Cq	NE	RE	Cq	Avg Ref Cq	delta Cq	NE	RE	Cq	Avg Ref Cq	delta Cq	NE	RE
5 dpf	29.67	20.87	-8.80	2.2E-03	0.28	25.33	20.98	-4.35	4.9E-02	19.05	25.11	20.73	-4.38	4.8E-02	2.74
7 dpf	29.12	20.77	-8.35	3.1E-03	0.38	30.05	21.01	-9.04	1.9E-03	0.74	24.60	20.74	-3.86	6.9E-02	3.94
11 dpf	30.95	23.01	-7.94	4.1E-03	0.51	32.30	23.18	-9.12	1.8E-03	0.70	26.30	23.15	-3.15	1.1E-01	6.44
28 dpf	29.63	22.61	-7.02	7.7E-03	0.97	30.73	22.92	-7.81	4.5E-03	1.74	27.04	22.57	-4.47	4.5E-02	2.57
adult (Calibrator)	26.71	19.74	-6.97	8.0E-03	1.00	28.64	20.04	-8.60	2.6E-03	1.00	25.35	19.51	-5.84	1.7E-02	1.00

Relative to SM-22 and Normalized to Reference Genes

comparing one gene to another	Kita					Kitb				
	Cq	Avg Ref Cq	delta Cq	NE	RE	Cq	Avg Ref Cq	delta Cq	NE	RE
5 dpf	32.05	20.99	-11.06	4.7E-04	0.0098	35.58	20.95	-14.63	3.9E-05	0.0008
7 dpf	31.27	20.89	-10.38	7.5E-04	0.0109	36.08	20.86	-15.22	2.6E-05	0.0004
11 dpf	32.33	23.20	-9.13	1.8E-03	0.0158	34.34	23.18	-11.16	4.4E-04	0.0039
28 dpf	33.70	22.66	-11.04	4.7E-04	0.0105	32.40	22.73	-9.67	1.2E-03	0.0273
adult	30.30	19.88	-10.43	7.3E-04	0.0416	30.75	19.86	-10.90	5.3E-04	0.0300

comparing one gene to another	Kitla					Kitlb					Sm-22				
	Cq	Avg Ref Cq	delta Cq	NE	RE	Cq	Avg Ref Cq	delta Cq	NE	RE	Cq	Avg Ref Cq	delta Cq	NE	RE
5 dpf	29.67	20.87	-8.80	2.2E-03	0.0467	25.33	20.98	-4.35	4.9E-02	1.0210	25.11	20.73	-4.38	4.8E-02	1.00
7 dpf	29.12	20.77	-8.35	3.1E-03	0.0444	30.05	21.01	-9.04	1.9E-03	0.0275	24.60	20.74	-3.86	6.9E-02	1.00
11 dpf	30.95	23.01	-7.94	4.1E-03	0.0362	32.30	23.18	-9.12	1.8E-03	0.0160	26.30	23.15	-3.15	1.1E-01	1.00
28 dpf	29.63	22.61	-7.02	7.7E-03	0.1715	30.73	22.92	-7.81	4.5E-03	0.0992	27.04	22.57	-4.47	4.5E-02	1.00
adult	26.71	19.74	-6.97	8.0E-03	0.4564	28.64	20.04	-8.60	2.6E-03	0.1471	25.35	19.51	-5.84	1.7E-02	1.00

Appendix 2.12: Experiment 2 Summary

Relative to Adult Expression and Normalized to Reference Genes

temporal expression for individual genes	Kita					Kitb				
	Cq	Avg Ref Cq	delta Cq	NE	RE	Cq	Avg Ref Cq	delta Cq	NE	RE
5 dpf	30.10	19.70	-10.40	7.4E-04	7.1E-01	32.05	19.63	-12.42	1.8E-04	5.3E+00
7 dpf	29.07	19.63	-9.44	1.4E-03	1.4E+00	33.88	19.51	-14.37	4.7E-05	1.4E+00
11 dpf	29.23	19.73	-9.50	1.4E-03	1.3E+00	33.25	19.61	-13.64	7.8E-05	2.3E+00
28 dpf	31.60	21.03	-10.57	6.6E-04	6.3E-01	35.00	21.02	-13.98	6.2E-05	1.8E+00
adult (Calibrator)	30.38	20.47	-9.91	1.0E-03	1.00	35.28	20.46	-14.83	3.4E-05	1.00

temporal expression for individual genes	Kitla					Kitlb					Sm-22			
	Cq	Avg Ref Cq	delta Cq	NE	RE	Cq	Avg Ref Cq	delta Cq	NE	RE	Cq	Avg Ref Cq	delta Cq	NE
5 dpf	29.34	19.69	-9.65	1.2E-03	5.6E-01	33.21	19.72	-13.49	8.7E-05	1.4E+00	25.00	19.65	-5.35	2.5E-02
7 dpf	29.21	19.60	-9.61	1.3E-03	5.8E-01	33.76	19.62	-14.14	5.6E-05	9.1E-01	24.10	19.62	-4.48	4.5E-02
11 dpf	27.75	19.69	-8.06	3.8E-03	1.7E+00	32.38	19.77	-12.61	1.6E-04	2.6E+00	23.70	19.71	-3.99	6.3E-02
28 dpf	29.54	21.07	-8.47	2.8E-03	1.3E+00	34.06	21.11	-12.95	1.3E-04	2.1E+00	24.02	21.08	-2.94	1.3E-01
adult (Calibrator)	29.24	20.43	-8.81	2.2E-03	1.00	34.53	20.52	-14.01	6.1E-05	1.00	24.47	20.51	-3.96	6.4E-02

Relative to SM-22 and Normalized to Reference Genes

comparing 1 gene to another	Kita					Kitb				
	Cq	Avg Ref Cq	delta Cq	NE	RE	Cq	Avg Ref Cq	delta Cq	NE	RE
5 dpf	30.10	19.70	-10.40	7.4E-04	3.0E-02	32.05	19.63	-12.42	1.8E-04	7.4E-03
7 dpf	29.07	19.63	-9.44	1.4E-03	3.2E-02	33.88	19.51	-14.37	4.7E-05	1.1E-03
11 dpf	29.23	19.73	-9.50	1.4E-03	2.2E-02	33.25	19.61	-13.64	7.8E-05	1.2E-03
28 dpf	31.60	21.03	-10.57	6.6E-04	5.1E-03	35.00	21.02	-13.98	6.2E-05	4.7E-04

comparing 1 gene to another	Kitla					Kitlb					Sm-22			
	Cq	Avg Ref Cq	delta Cq	NE	RE	Cq	Avg Ref Cq	delta Cq	NE	RE	Cq	Avg Ref Cq	delta Cq	NE
5 dpf	29.34	19.69	-9.65	1.2E-03	5.1E-02	33.21	19.72	-13.49	8.7E-05	3.5E-03	25.00	19.65	-5.35	2.5E-02
7 dpf	29.21	19.60	-9.61	1.3E-03	2.9E-02	33.76	19.62	-14.14	5.6E-05	1.2E-03	24.10	19.62	-4.48	4.5E-02
11 dpf	27.75	19.69	-8.06	3.8E-03	6.0E-02	32.38	19.77	-12.61	1.6E-04	2.6E-03	23.70	19.71	-3.99	6.3E-02
28 dpf	29.54	21.07	-8.47	2.8E-03	2.2E-02	34.06	21.11	-12.95	1.3E-04	9.7E-04	24.02	21.08	-2.94	1.3E-01

Appendix 3: Primer Optimization

Appendix 3.1: Primer Sequence and Accession

Name	Sequence (5'-3')	Accession
zf bactin f	CGAGCAGGAGATGGGAACC	b-actin 1: NM_131031
zf bactin r	CAACGGAAACGCTCATTGC	
beta actin RT- F	CGAGCTGTCTTCCCATCCA	b-actin 2: NM_181601
beta actin RT- R	TCACCAACGTAGCTGTCTTTCTG	
kitaf1	AACCGAGACGCAACTATCC	NM_131053.1
kitar1	CTCCTCCTGAGTGGCATTC	
kitbf1	TCAGGGAGGAATCACCATCAG	NM_001143918.1
kitbr1	AGCCGCACAACCAAGTTATAC	
kitlbf1	CATTAGGAAGAAGAGGTCGTTGTG	XM_677667.3
kitlbr1	ACTGGCGGAGGTGGAAGC	
kitla f1	AATCTCATGTGGCTCCTC	AY929068
kitla r1	GGACCTTCTTCTGGACTC	
kitla R2	AACCGTTTCGTTTCTCATTTG	AY929068
kitla F2	CAACACTGCCAATTCATCAAG	

sm22 F2	AGCAGGTCTCGCAGTTCC	AY934529
sm22 R2	GCCCAGAGCCATCAGAGTC	
rppo F	CTGAACATCTCGCCTTCTC	NM_131580
rppo R	TAGCCGATCCGCAGACACAC	
EF1alpha F	CTGGAGGAGGCCAGCTCAAACAT	FJ915061
EF1alpha R	ATCAAGAAGAGTAGTACCGCTAGCATTAC	
Rpl13 alpha F	TCTGGAGGACTGTAAGAGGTATGC	NM_212784 XM_703004
Rpl13 alpha R	AGACGCACAATCTTGAGAGCAG	

Gene	bactin rt	bactin zf	EF1alpha	Rpl13alpha	rppo
Temperature (°C)	C_q ± SD				
64	18.8 ± 0.05	22.2 ± 0.26	18.5 ± 0.08	18.8 ± 0.06	20.9 ± 0.08
63.5	18.6 ± 0.01	21.9 ±0.05	18.2 ± 0.01	18.6 ± 0.09	19.9 ± 0.01
62.3	18.4 ± 0.03	21.8 ±0.06	18.1 ± 0.05	18.4 ± 0.04	19.1 ± 0.18
60.4	18.3 ± 0.03	21.7 ± 0.06	18.0 ± 0.01	18.3 ± 0.01	18.5 ± 0.08
57.9	18.1 ± 0.06	22.2± 0.04	18.1 ± 0.26	18.2 ±0.00	18.2 ± 0.02
56.1	18.0 ± 0.04	21.9 ± 0.63	17.9 ± 0.04	18.1 ± 0.03	18.4 ± 0.44
54.8	18.0 ± 0.12	21.5 ± 0.12	17.9 ± 0.03	18.1 ±0.05	18.8 ± 0.28
54	18.1 ± 0.07		18.0 ± 0.04	18.2 ± 0.03	

Gene	kita	kitb	kitla	kitlb	sm22
Temperature (°C)	C_q ± SD				
64	30.9 ±0.00	27.4 ± 0.56	27.2 ± 0.84	27.6 ± 0.16	22.6 ± 0.30
63.5	30.7 ± 0.05	26.7 ± 0.08	26.4 ± 0.21	27.3 ± 0.01	22.2 ± 0.05
62.3	30.5 ± 0.49	26.7 ± 0.04	26.2 ± 0.19	27.4 ± 0.01	22.0 ± 0.17
60.4	30.3 ± 0.02	26.4 ± 0.09	25.9 ± 0.01	27.0 ± 0.06	21.8 ± 0.03
57.9	30.1 ± 0.19	26.3 ± 0.01	25.7 ± 0.09	26.9 ± 0.02	21.8 ± 0.05
56.1	30.3 ± 0.18	26.3 ± 0.15	25.6 ± 0.11	26.7 ± 0.04	21.6 ± 0.06
54.8	30.0 ± 0.20	26.3 ± 0.25	25.6 ± 0.07	26.5 ± 0.03	21.6 ± 0.05
54		26.5 ± 0.32	25.6 ± 0.09	26.5 ± 0.29	21.7 ± 0.05

Appendix 3.2: Temperature Gradient Data

Appendix 3.3: Standard Curve Data

B-Actin RT

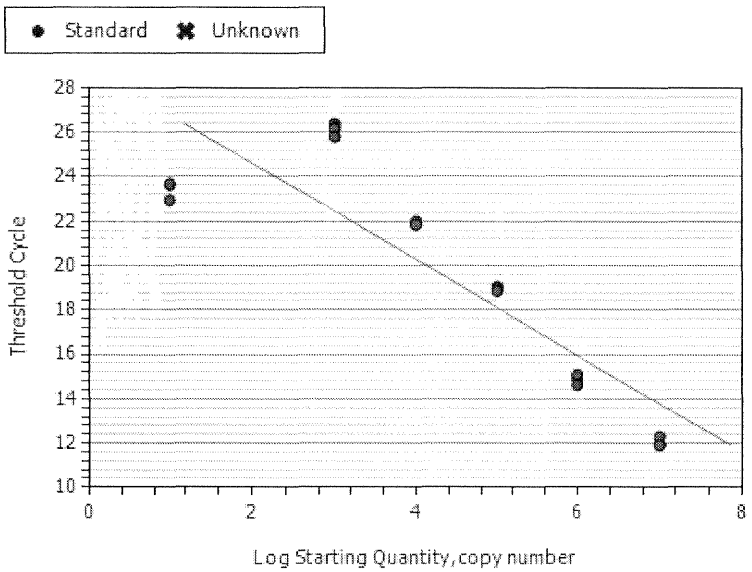

Fluor	PCR Efficiency(%)	R Squared	Slope	y-Intercept
SYBR	188.8	0.772	-2.171	28.969

EF1alpha

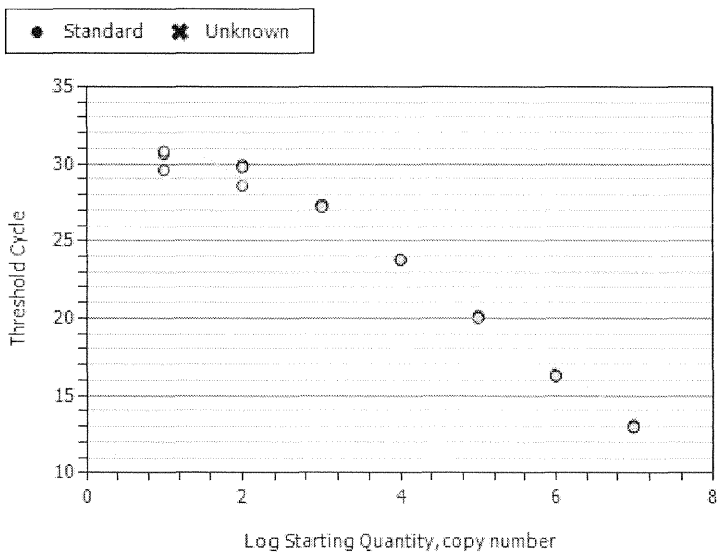

Fluor	PCR Efficiency(%)	R Squared	Slope	y-Intercept
SYBR2	112.8	0.973	-3.049	35.093

RPL13alpha

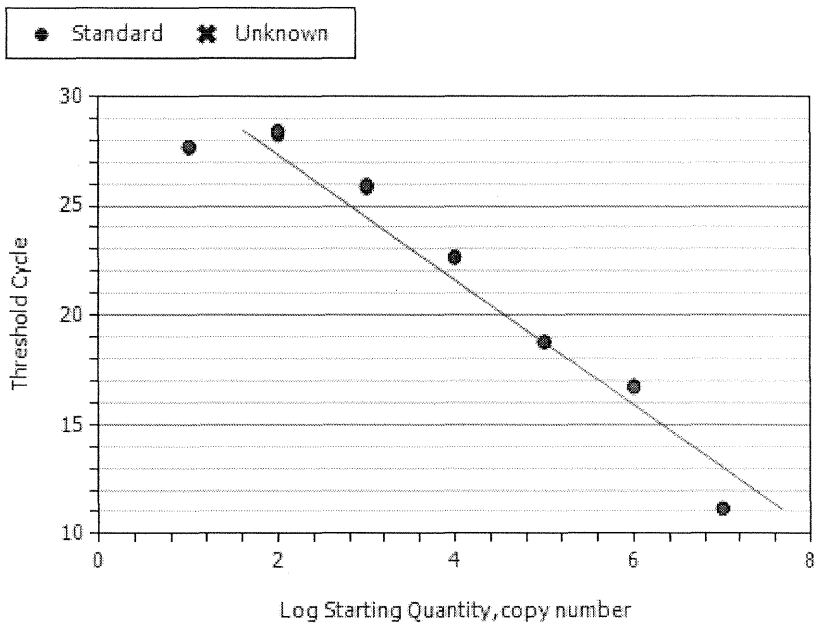

Fluor	PCR Efficiency(%)	R Squared	Slope	y-Intercept
SYBR1	124.0	0.939	-2.855	33.029

Kita

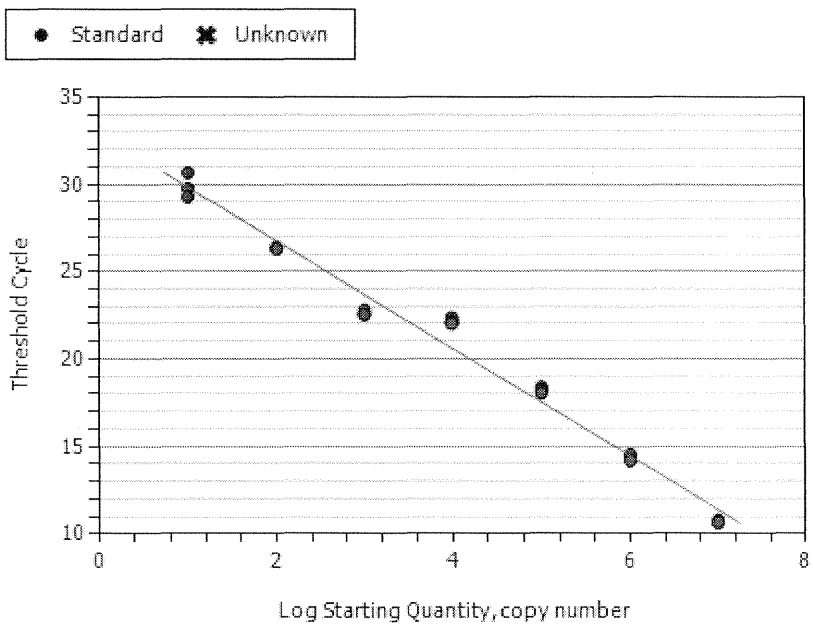

Fluor	PCR Efficiency(%)	R Squared	Slope	y-Intercept
SYBR	111.5	0.981	-3.074	32.906

Kitb

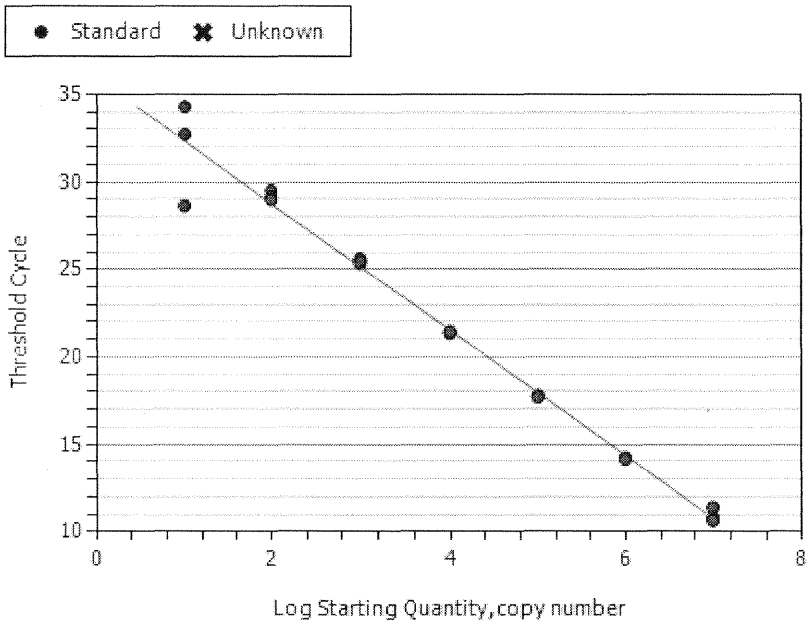

Fluor	PCR Efficiency(%)	R Squared	Slope	y-Intercept
SYBR1	89.8	0.982	-3.592	35.929

Kitla

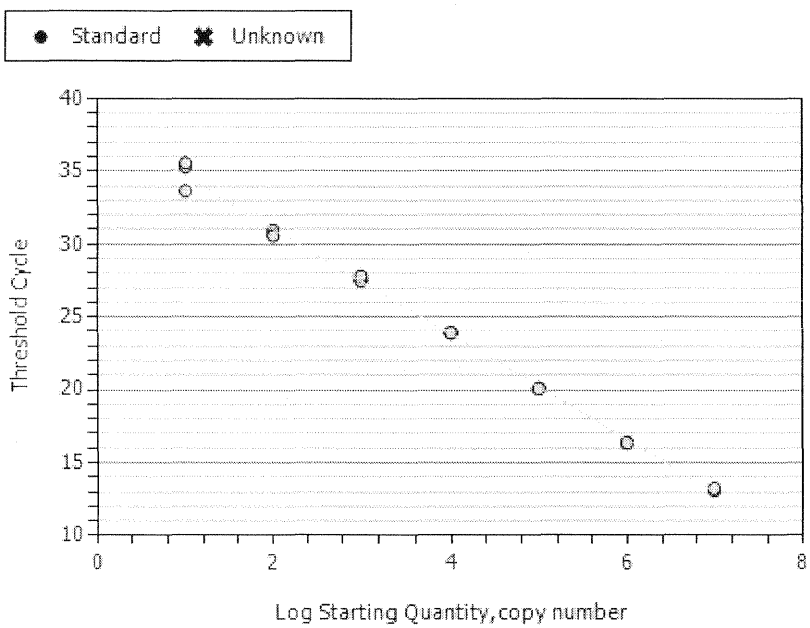

]				/-Intercept
SYBR2	89.0	0.997	-3.618	38.293

Kitlb

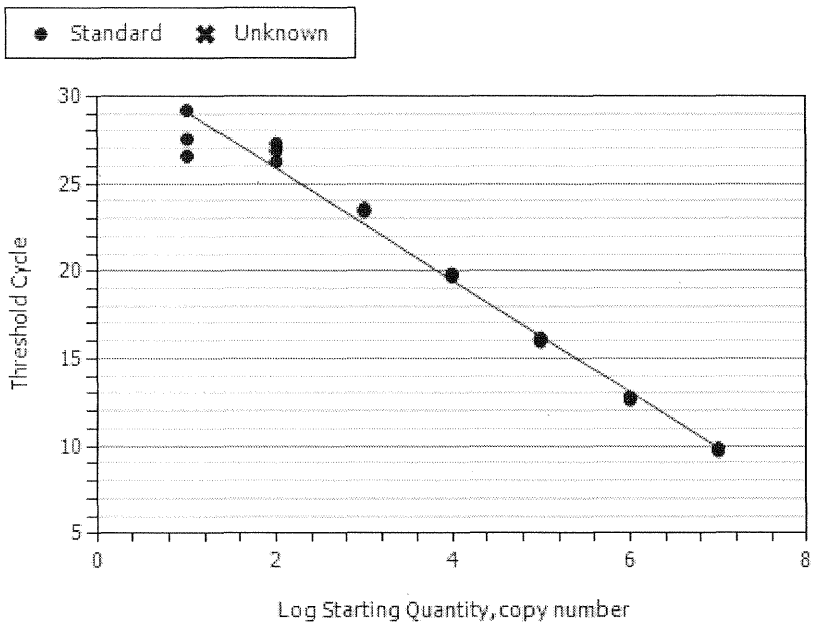

Fluor	PCR Efficiency(%)	R Squared	Slope	y-Intercept
SYBR3	105.5	0.983	-3.197	32.282

SM-22

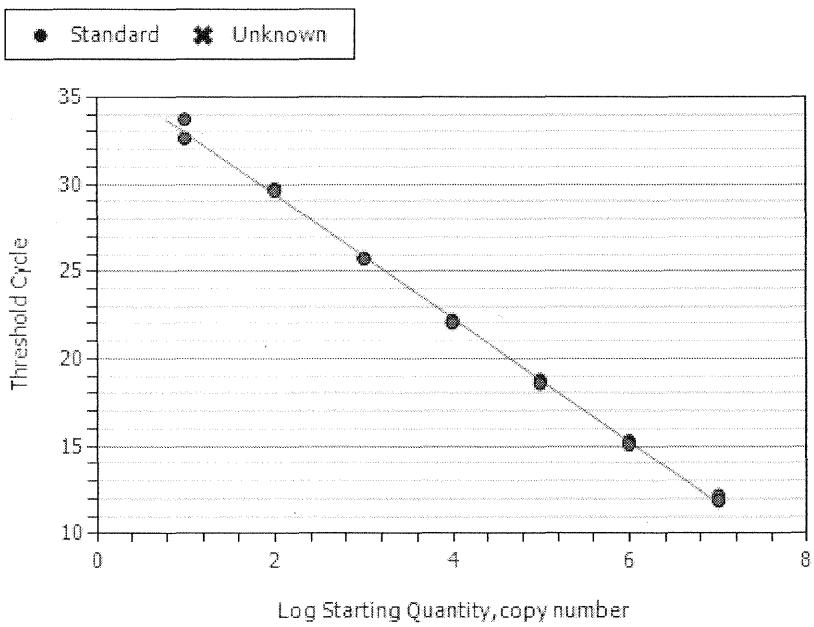

Fluor	PCR Efficiency(%)	R Squared	Slope	y-Intercept
SYBR	91.6	0.998	-3.540	36.500

Appendix 4: RNA Quality Data

Appendix 4.1: Experiment 1, Adult Samples

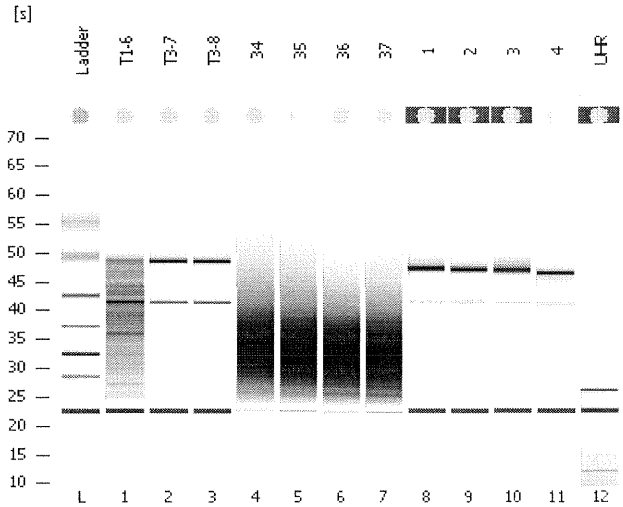

Nano Chip

48s: 28S Ribosomal Subunit

42s: 18S Ribosomal Subunit

Samples:

Lane 8: Adult 1 (6/4/10)

Lane 9: Adult 2 (6/4/10)

Adult 1 (6/4/10)

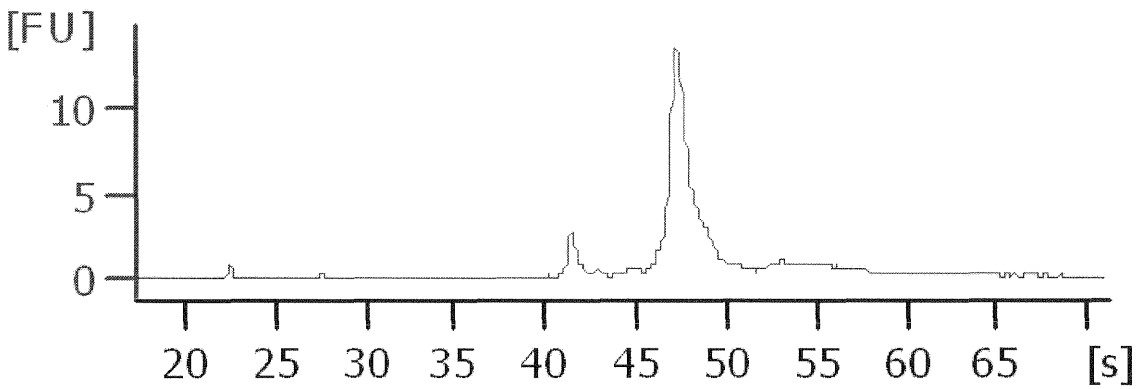

Adult 2 (6/4/10)

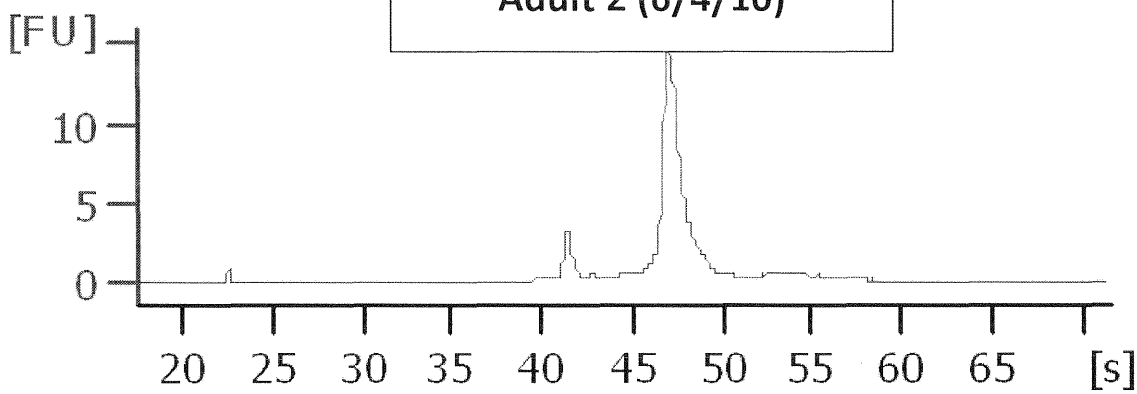

Appendix 4.2: Experiment 1, 28 dpf

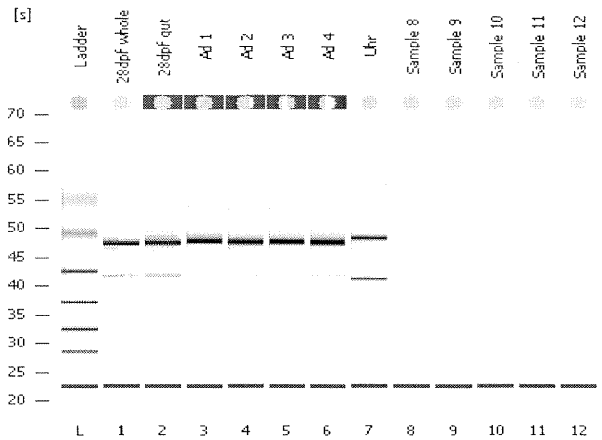

Nano Chip

48s: 28S Ribosomal Subunit

42s: 18S Ribosomal Subunit

Samples:

Lane 2: 28dpf gut (9/24/10)

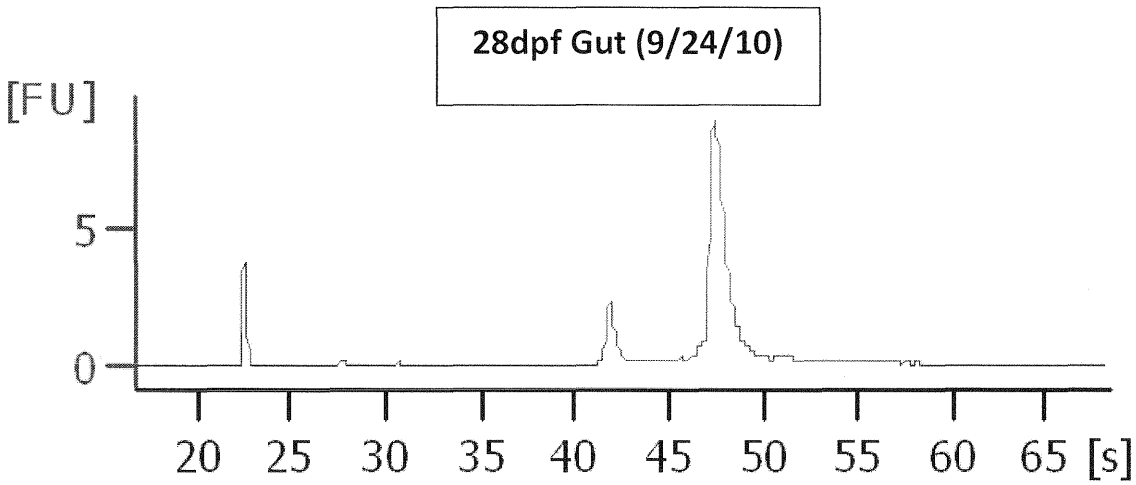

Appendix 4.3: Experiment 1 and 2, developmental time points

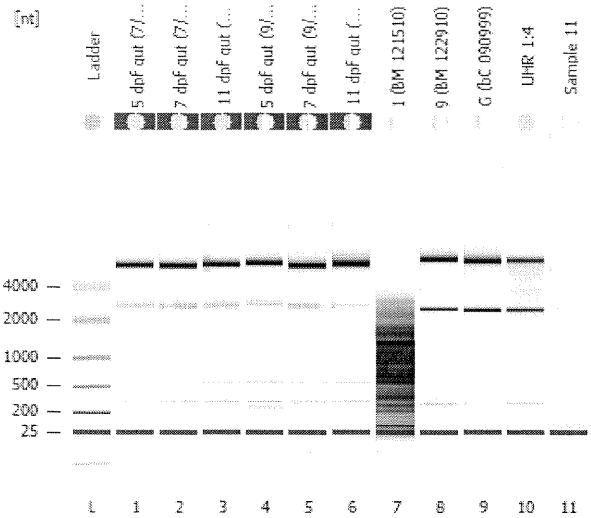

Pico Chip

5000nt: 28S Ribosomal Subunit
3000nt: 18S Ribosomal Subunit
Samples:

- Lane 1: 5dpf gut (7/20/10) Experiment 1
- Lane 2: 7dpf gut (7/22/10) Experiment 1
- Lane 3: 11dpf gut (7/12/10) Experiment 1
- Lane 4: 5dpf gut (9/1/10) Experiment 2
- Lane 5: 7dpf gut (9/3/10) Experiment 2
- Lane 6: 11dpf gut (9/7/10) Experiment 2

5dpf gut (7/20/10) Experiment 1

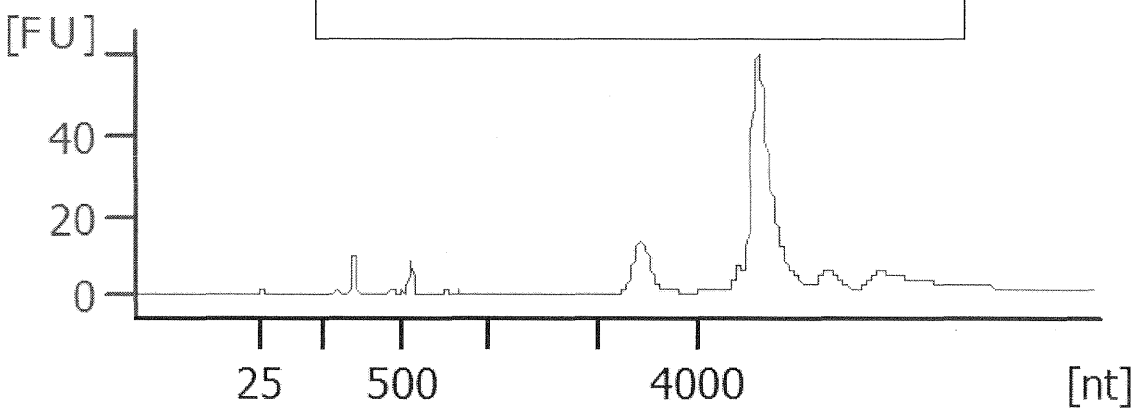

7dpf gut (7/22/10) Experiment 1

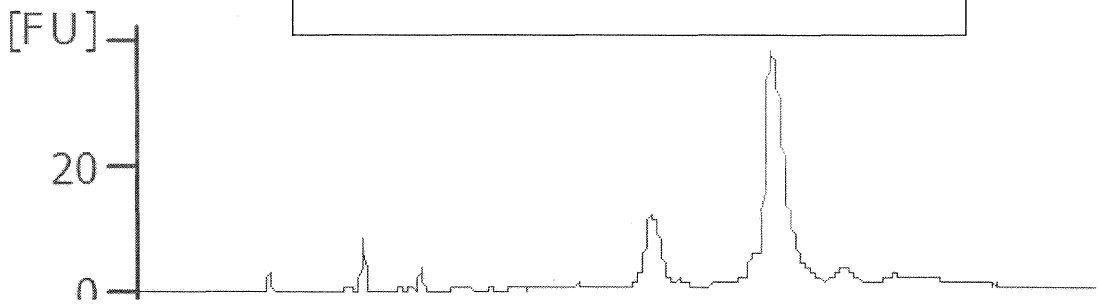

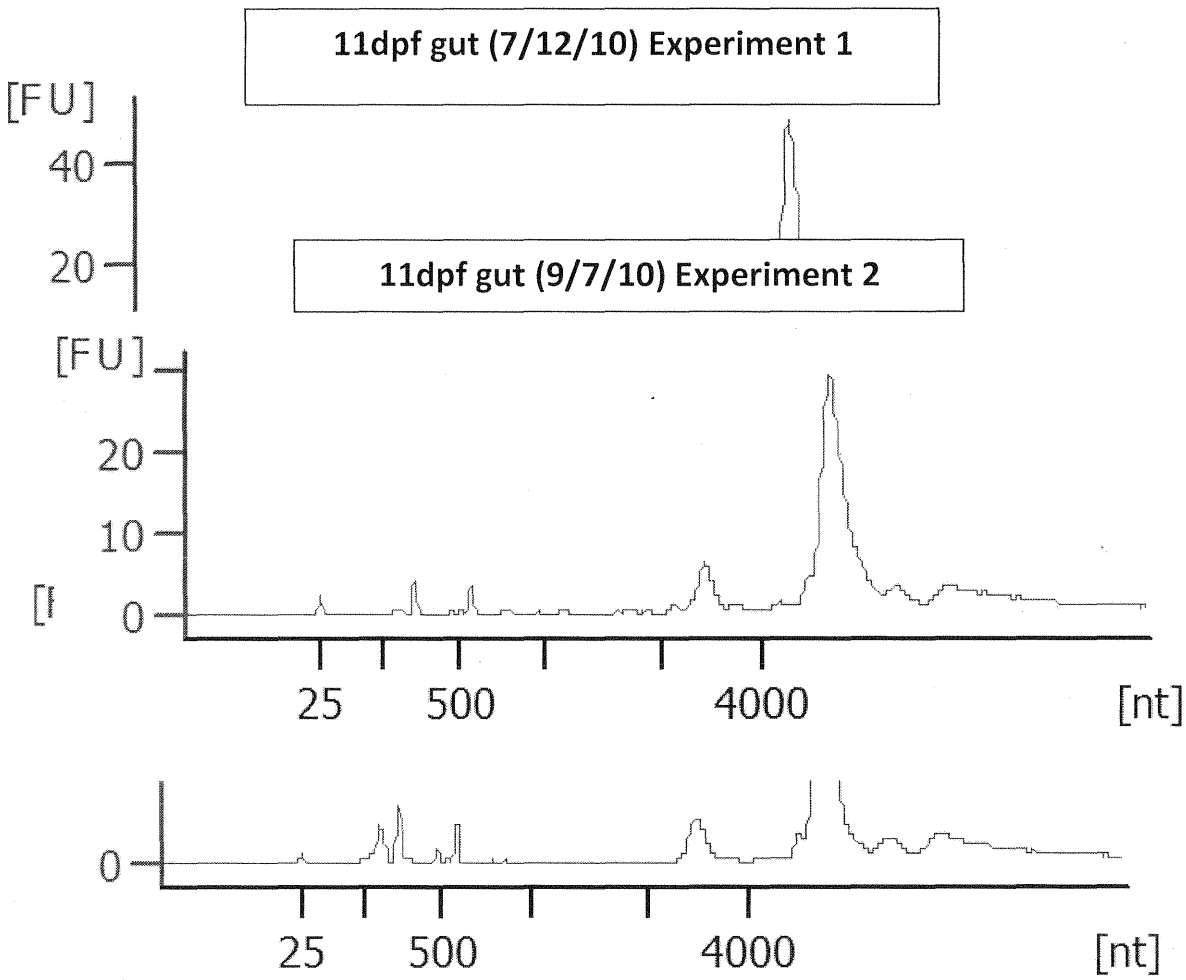
11dpf gut (7/12/10) Experiment 1
[FU]
40
20
11dpf gut (9/7/10) Experiment 2
[FU]
20
10
0
25
500
4000
[nt]
0
25
500
4000
[nt]

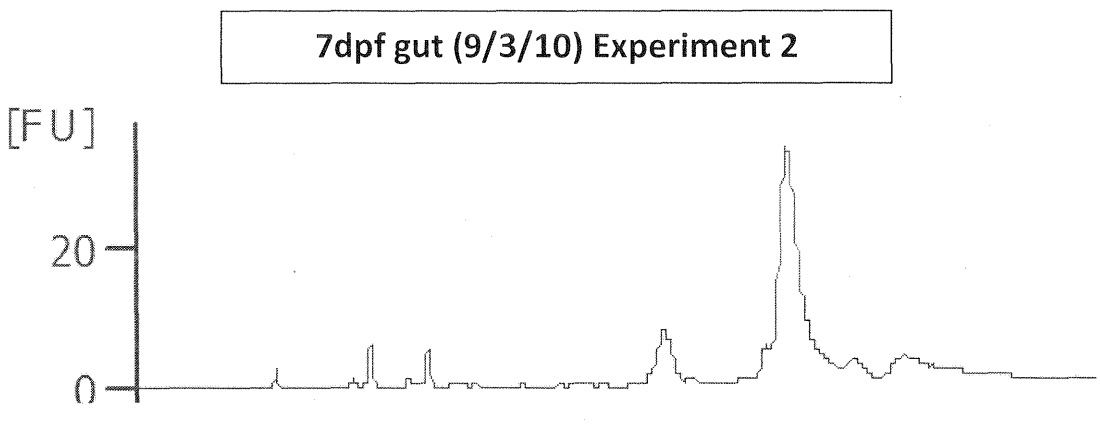
7dpf gut (9/3/10) Experiment 2
[FU]
20
0

Appendix 4.4 Experiment 2, 28dpf and adult

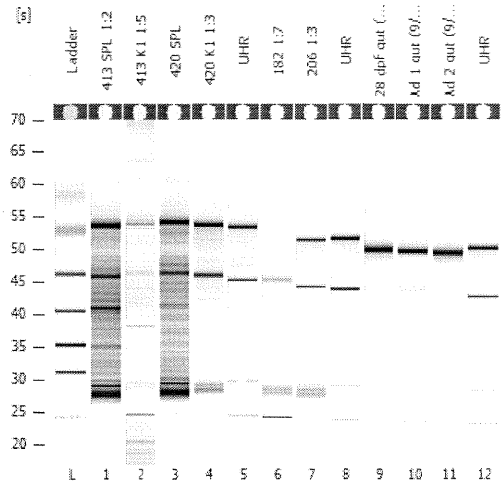

Nano Chip

48s: 28S Ribosomal Subunit

42s: 18S Ribosomal Subunit

Samples:

Lane 9: 28dpf (9/24/10)

Lane 10: Adult 1 (9/24/10)

Lane 11: Adult 2 (9/24/10)

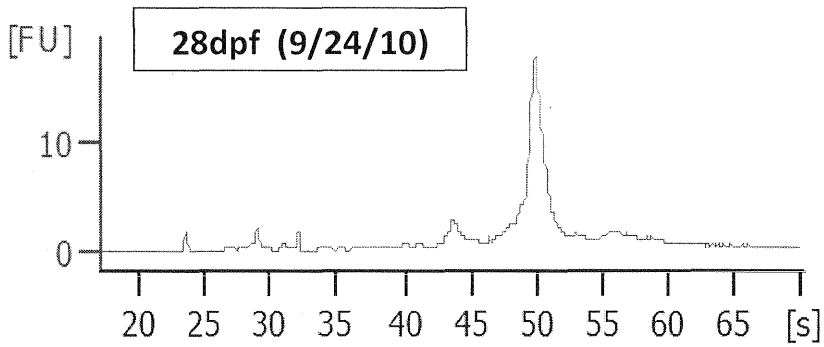

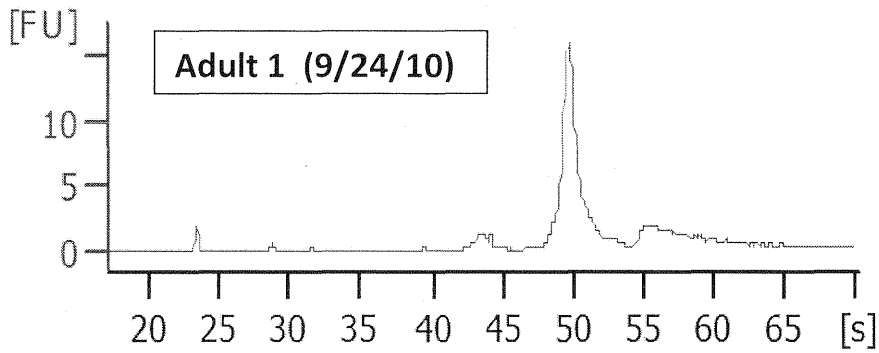

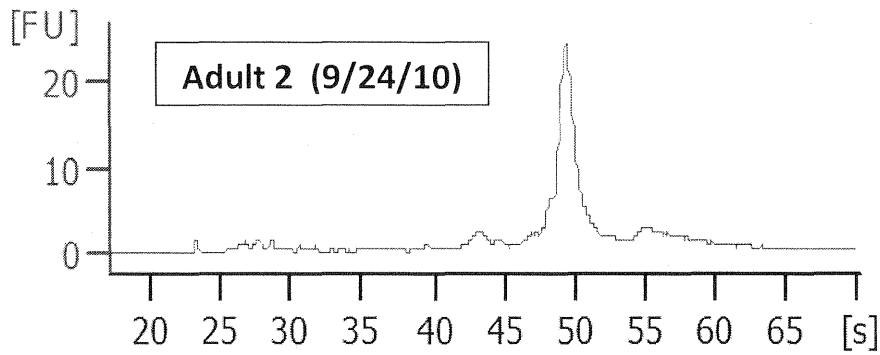

Appendix 5: Real-Time Data

Appendix 5.1: Experiment 1 Temporal Expression

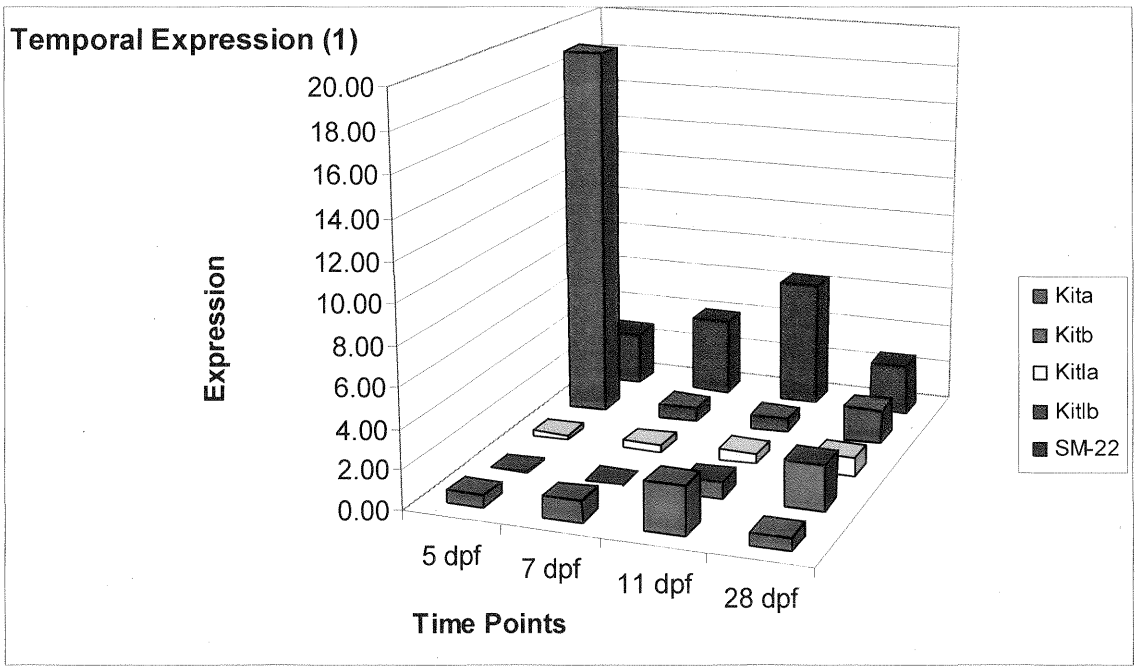

Figure 5.1 shows the temporal expression of Kita, Kitb, Kitla, and Kitlb at 5,7,11,and 28dpf. Temporal expression is normalized to a panel of reference genes and is relative to adult expression at the same time point. Experiment 1 data was not used in this thesis because of many outlaying data points suggesting pippeting error.

Appendix 5.2: Experiment 1 Relative Expression

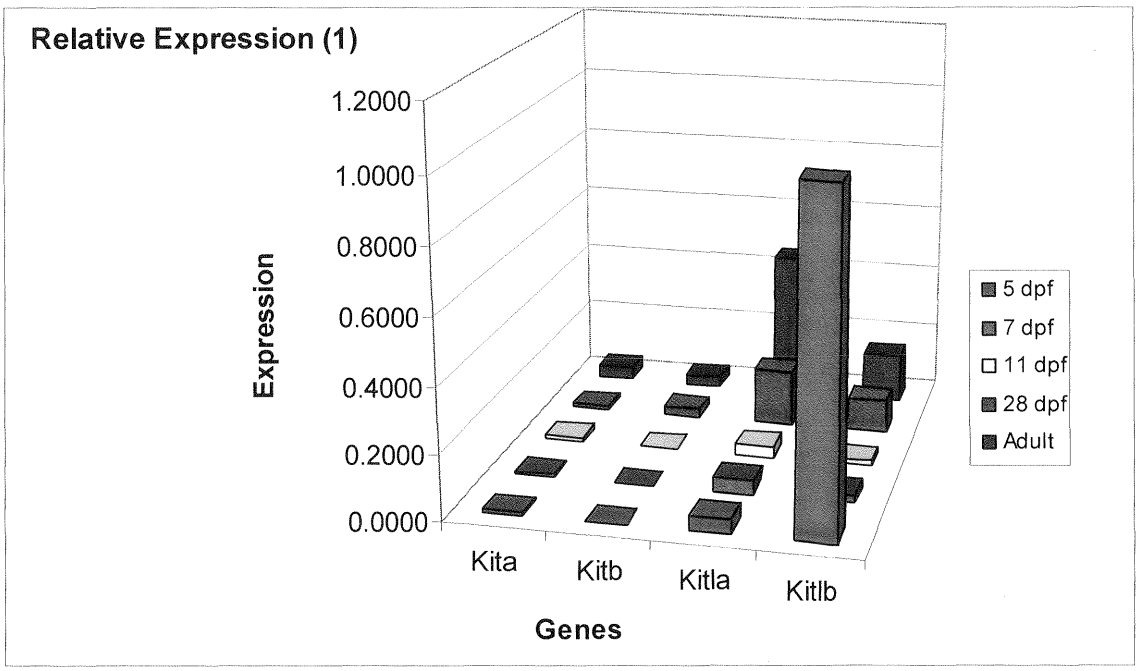

Figure 5.2 shows the relative expression at 5, 7, 11, 28dpf and adult time points for Kita, Kitb, Kitla, and Kitlb. Relative expression was determined by normalizing to a panel of reference genes and is relative to SM-22. Experiment 1 data was not used in this thesis because of many outlaying data points suggesting pippeting error.